Earth Sciences
2022; 11(6): 338-354
http://www.sciencepublishinggroup.com/j/earth
doi: 10.11648/j.earth.20221106.11
ISSN: 2328-5974 (Print); ISSN: 2328-5982 (Online)

Last Paleozoic Subduction in Eastern Junggar: Evidence from Geochemistry, Geochronology and Petrogenesis of Carboniferous Volcanic Rocks

Feng Zhang[1], Tao Xu[1], Yingchuan Lu[2]

[1]Research Center of Applied Geology, China Geophysical Survey, Chengdu, China

[2]Center for Geophysical Survey, China Geophysical Survey, Langfang, China

Email address:
ZF75738635@163.com (Feng Zhang)

To cite this article:
Feng Zhang, Tao Xu, Yingchuan Lu. Last Paleozoic Subduction in Eastern Junggar: Evidence from Geochemistry, Geochronology and Petrogenesis of Carboniferous Volcanic Rocks. *Earth Sciences*. Vol. 11, No. 6, 2022, pp. 338-354. doi: 10.11648/j.earth.20221106.11

Received: May 13, 2022; **Accepted**: May 30, 2022; **Published**: November 4, 2022

Abstract: The Carboniferous Batamayineishan volcanic rocks in Eastern Junggar are widely distributed on a huge scale. Studies on geochemistry, geochronology and petrogenesis of these volcanic rocks show that: (1) they have complex volcanic rock types with basalt - andesite - dacite - rhyolite assemblages and are of high-K calc-alkaline series, with enrichment of large ion lithophile elements (LILE) (Sr, K, Rb, Ba, Th) and light rare earth elements (LREE) and depletion of high field strength elements (HFSE) (Nb, Ta, Ti) and heavy rare earth elements (HREE). Besides, the initial $^{87}Sr/^{86}Sr$ and $^{143}Nd/^{144}Nd$ ratios are low and the ε_{Nd} (t) values mostly vary from 3.0 to 6.2. All these features suggest that the volcanic rocks were formed in the immature back-arc basin related to subduction; (2) The Batamayineishan volcanic rocks may be produced by the multi-source materials interaction of young lower crust and deep mantle materials which are mainly composed of the Paleozoic residual oceanic crust and island arc system. The basalts were dominantly derived from the depleted mantle, and the crust-mantle magmatism and the homogenization of the Sm-Nd isotope system have occurred with a small amount of young crustal materials in the magma source. Their formation is likely related to the partial melting of the overlying mantle wedges caused by the fluids generated by the metamorphism and dehydration of subducted sediments and/or subducted oceanic crust. However, the acidic volcanic rocks are the result of the mixing of a small amount of mantle-derived magma undergoing strong crystallization differentiation and a mass of crust-derived materials; (3) The Sm-Nd isochron age of the basalts is (319.7±5.9) Ma, which is consistent with the regional tectonic setting and the evidence from fossils in Batamayineishan Formation, and represents the eruption age of the Batamayineishan volcanic rocks. In summary, we consider that the subduction of the Paleo-Asian Ocean continued in Eastern Junggar around 320Ma, and its final closure time should be between 320 Ma and 310 Ma. During this process, the volcanic magmatisms in Eastern Junggar were very intense and involved abundant mantle-derived materials, implying that Eastern Junggar has a superior prospecting potential.

Keywords: Volcanic Rocks, Geochemistry, Back-arc Basin, Carboniferous, Batamayineishan Formation, Eastern Junggar

1. Introduction

The Junggar Basin, located between the Siberian plate and the Tarim plate, is an important part of the Central Asian Orogenic belt and belongs to the Kazakhstan-Junggar plate [1]. The ophiolite belt and igneous rocks around the basin provide a favorable material basis for studying the regional tectonic evolution in Western China and even whole Central Asia.

Carboniferous was an important period of tectonic regime transition in Junggar [2], with intense volcanic magmatism and extensive volcanic rocks outcropping, particularly in Eastern Junggar. In recent years, with the deepening of geological surveys, oil and gas and solid mineral resources have been discovered in carboniferous volcanic rocks in Eastern Junggar, highlighting superior prospecting potential in this area. Among the Carboniferous volcanic rocks, those in Batamayineishan Formation, outcropped widely on a huge

scale and preserved well, have attracted the attention of some geologists. However, Up to now, the studies on them are still at a relatively low level, and there are as ever a few arguments about their formation age and tectonic setting, including formed in Early Carboniferous [3, 4] or Late Carboniferous [5-11], and post-orogenic extension setting related to collisional orogeny [3, 10, 11, 12-14] or island arc setting related to the subduction of oceanic crust [15-17], etc.

The Kalamaili ophiolitic belt, with Batamayineishan volcanic rocks occurred widely, is located on the northeastern margin of Junggar Basin. It can be linked to the Darabut ophiolite belt in Western Junggar and is considered a remnant of the Late Paleozoic Junggar Ocean [1]. The Junggar Ocean has been identified as an important branch in the north and a stage production of Paleozoic evolution of the Paleo-Asian ocean [1, 8]. But there are still some controversies about the final closure time of it, such as Devonian [19], Early Carboniferous [4, 8, 10, 11, 20], Late Carboniferous [6, 7, 11, 21, 22], Permian [15, 24, 25] and so on. Therefore, the studies on the Volcanic rocks in Batamayineishan Formation will be of great significance to constraining the final closure time of Junggar Ocean and interpreting the Paleozoic tectonic evolution of the Paleo-Asian Ocean and Western China, even the whole of Central Asia.

In this contribution, we present detailed petrology, petrochemistry, Sr-Nd isotopic composition, and Sm-Nd geochronology for the Batamayineishan volcanic rocks in Kalamaili ophiolitic belt. These new data provide insights into the formation age, tectonic setting, and petrogenesis of Batamayineishan volcanic rocks, constrain the final closure time of the Junggar Ocean and afford a theoretical basis for prospecting in Kalamaili.

2. Geological Setting and Petrographic Characteristics of Volcanic Rocks

The Kalamaili ophiolite belt is located in the Kalamaili Mountains, on the north of Batamayineishan Mountains. It is controlled by Kalamaili deep fault and distributed in NWW. The exposed stratas in and around this belt are relatively simple, mainly the late Paleozoic Devonian and the Carboniferous (Figure 1). The Devonian, dominated by the Middle Devonian, is a suite of shallow-coastal facies clastic rock formations with extremely weak volcanic activity. The Carboniferous can be divided, from base to top, into Nanmingshui Formation, Qingshui Formation, Songkarsu Formation, Batamayineishan Formation, and Shuangjingzi Formation. Except for the Batamayineishan Formation, the volcanic rocks in other Carboniferous strata are not developed, and most of them belong to shallow marine facies or marine-terrigenous clastic sedimentary rock series. The Batamayineishan Formation was nominated by the Regional geological Survey Battalion of Xinjiang Geological Bureau during the 1:200,000 regional geological and mineral survey. This formation site is located near the Batamayineishan mountains close to the Karamaili ophiolite belt. It is the main strata of volcanic rocks in the northeastern margin of Junggar basin, mainly manifested as a set of basic-acid volcanic rock and volcanic clastic rock series. Among them, the volcanic rocks are composed of basalt, andesite, dacite, rhyolite and perlite, etc., with thousands of meters of thickness and obvious multi-stage, intermittent eruption characteristics. Similar features were discovered in Kalamaili ophiolite zone, where the rock types are mainly basalt, basaltic andesite, pyroxene andesite, andesite, and rhyolite. Their petrography is described by the following:

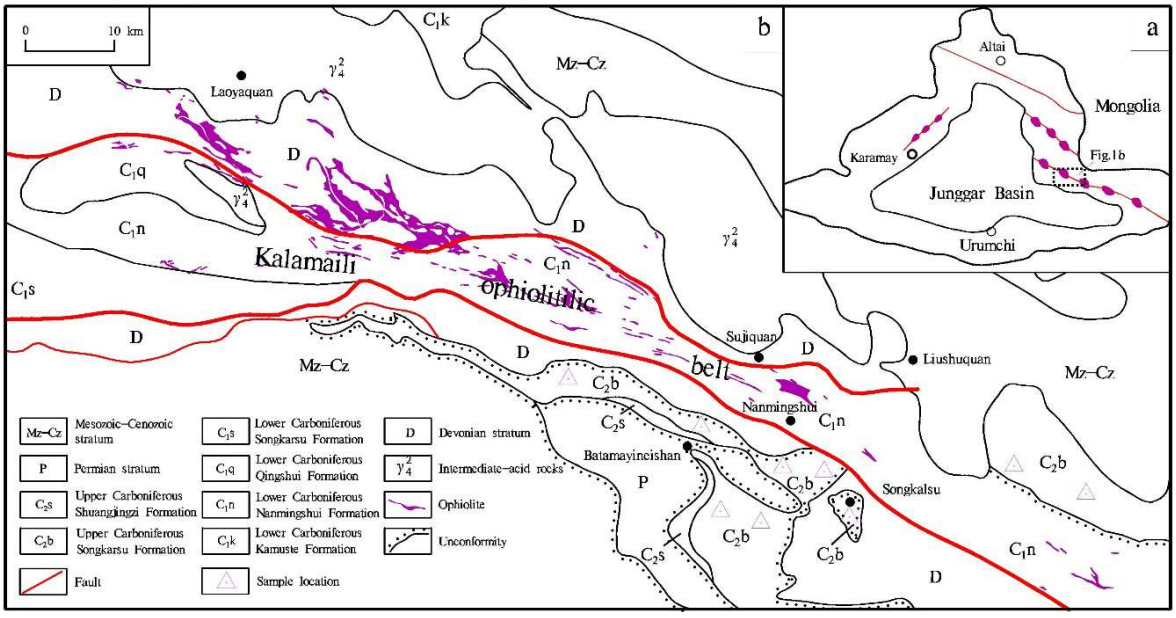

Figure 1. *(a) Geological map of Xinjiang. (b) Sketch geological map of Kalamaili in Eastern Junggar.*

The basalt is black, light gray-green, and has massive structure and porphyritic texture. The phenocrysts mainly consist of plagioclase (20%) and pyroxene (1~2%), which are most subhedral platy crystals, commonly 1~2 mm in size, and distributed disorderly. The plagioclase and pyroxene phenocrysts are respectively replaced by chlorite, sericite,

calcite chlorite, sericite and tremolite. The matrix with an intergranular texture is mainly composed of subhedral platy plagioclase and subhedral-anhedral columnar pyroxene. Among them, the plagioclase is generally 0.1~0.2 mm in size and distributed disorderly, ordinarily replaced by sericite. The pyroxene is generally 0.05~0.1 mm in size, set in the gaps of plagioclase grains, and ordinarily replaced by chlorite and tremolite (Figure 2a).

The Basaltic andesite is dark gray, light green, and grayish green in color and shows the amygdaloidal structure and porphyritic texture. The phenocrysts are subhedral platy plagioclase, generally 0.5~1 mm in size, cribriform erosion in part, and a content of 10~15%. The matrix with a porphyritic texture consists of microcrystalline subhedral platy plagioclase (50~55%) and subhedral-anhedral granular pyroxene (35~40%). Among them, the plagioclase is generally 0.1~0.2 mm in size and a small amount have been replaced by calcite and chlorite. The pyroxene is commonly 0.05~0.1 mm in size, set in the gaps of plagioclase grains and ordinarily replaced by chlorite and calcite (Figure 2a). The amygdala mainly consists of chlorite and calcite, with an irregular shape, generally, 0.2~0.5 mm in size and 5% in content (Figure 2b).

The pyroxene andesite is Dark grey, light grey-green, with a massive structure and a porphyritic texture. The phenocrysts are composed of subhedral crystal plagioclase (10~15%) and pyroxene (1~5%). The plagioclase crystals present platy in shape and the phenomenon of cribriform erosion is common. The pyroxene crystals are columnar and most replaced by chlorite and calcite. The matrix pyroxene andesite is a pilotaxitic texture and consists of plagioclase (60~65%) and pyroxene (25~30%), of which a small amount of the plagioclase with subhedral platy and the pyroxene with subhedral column have occurred chloritization and calcilization (Figure 2c).

The andesite is grayish-black and light grayish-green, amygdaloidal structure and porphyritic texture. The phenocrysts are plagioclase with subhedral platy, commonly 1 mm in size and less 1% in content, which have been strongly replaced by chlorite and calcite. The matrix is pilotaxitic texture and composed of plagioclase (more than 95%) and pyroxene (1~5%). The matrix plagioclase is subhedral platy, generally 0.1~0.2 mm in size and usually replaced by sericite, calcite and chlorite. The matrix pyroxene is subhedral-anhedral granular, generally 0.01~0.05 mm in size, and ordinarily replaced by chlorite, biotite and quartz. The amygdales, with commonly 0.01~0.05 mm in size, scattered in distribution and similar to ellipse and irregular in shape, consist of calcite and siliceous (primarily chalcedony) (2~20%) (Figure 2d).

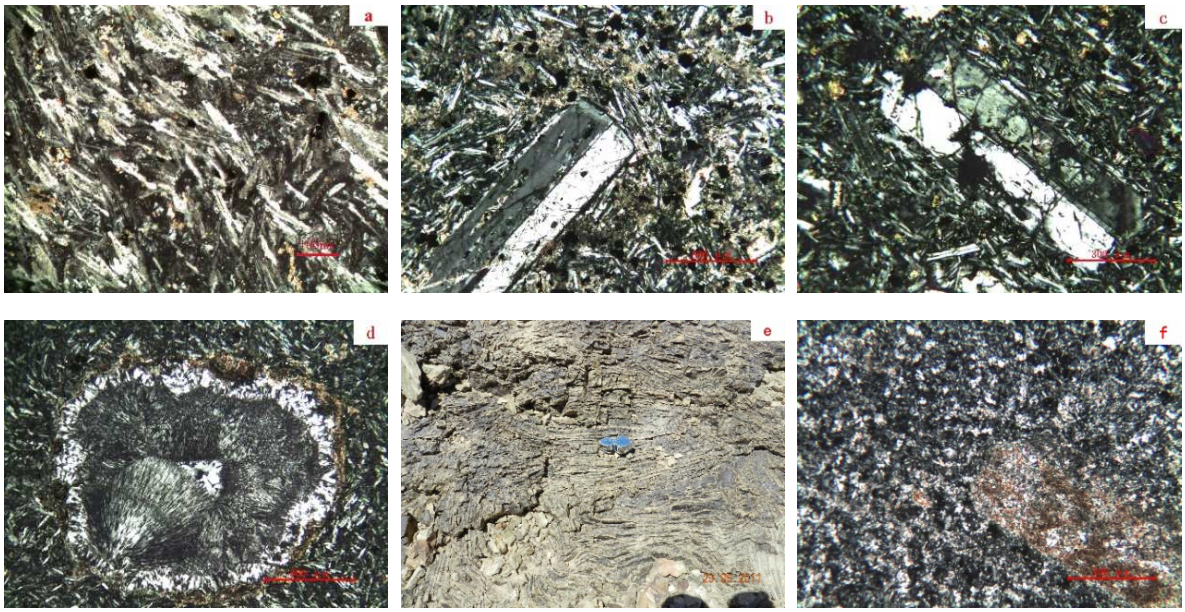

(a) Altered basalt (+); (b) Basaltic andesite (+); (c) Pyroxene andesite (+); (d) Amygdaloidal andesite (+); (e) Rhyolite; (f) Rhyolite (+).

Figure 2. *Petroeranhic characteristics of Carboniferous volcanic rocks of Kalamaili in Eastern Junggar.*

The rhyolite is mostly gray-white, showing the massive structure, rhyolitic structure and vesicular structure. The phenocrysts are plagioclase (1~5%) with subhedral platy, commonly 0.5~1 mm in size and scattered in distribution, and generally replaced by sericite, tourmaline. The matrix is composed of microfelsitic-microcrystalline plagioclase (40~55%), K-feldspar (30%) and quartz (25~30%). Among them, the plagioclase is subhedral-anhedral granular, generally 0.01~0.03 mm in size and ordinarily replaced by chlorite, the matrix K-feldspar is also subhedral-anhedral granular, and the quartz is only anhedral granular (Figure 2e, Figure 2f).

3. Analysis Method

Based on the hand specimen and microscopic observation, we selected the fresh volcanic rocks with fewer almonds as samples. And then all of the samples were removed the weathered surfaces, broken into rock fragments, dried and ground in a clean agate mill to the size of 200 mesh for geochemistry analyses. The whole-rock major and trace element analyses were performed at the Institute of Geophysical and Geochemical Exploration, Chinese Academy

of Geological Sciences. Major elements were determined by an X-Ray Fluorescence spectrometry (XRF) with a precision better than 1% and the content of FeO was obtained by the volumetric method (VOL). Trace elements were measured by an Inductively Coupled Plasma Mass Spectrometry (ICP-MS) and an X-Ray Fluorescence spectrometry (XRF). Rare earth elements were analyzed by an Inductively Coupled Plasma Mass Spectrometry (ICP-MS). The analytical accuracies for the trace elements are mostly better than 5%. As shown in Table 1, the loss on ignition (LOI) values for the samples, except SD04, SD05 and SD11, are between 0.61% and 7.29% and less than 2.5%, which are consistent with the microscopic observations. These indicate that the volcanic rock samples in this study were weakly affected by late hydrothermal alteration and the resulting data can be used for the analysis and discrimination of tectonic setting and petrogenesis.

Rb-Sr and Sm-Nd isotopic analyses were performed at the Isotope Dating Laboratory of Tianjin Institute of Geology and Mineralogy using a TRITON thermal ionization mass spectrometer. The concentrations of Rb, Sr, Sm, and Nd were determined by an isotope dilution method. All of the obtained $^{86}Sr/^{88}Sr$, $^{149}Sm/^{152}Sm$ and $^{146}Nd/^{144}Nd$ ratios were normalized to $^{86}Sr/^{88}Sr=0.119400$, $^{149}Sm/^{152}Sm=0.516858$ and $^{146}Nd/^{144}Nd = 0.721900$, respectively, and the Rayleigh's law were adopted for their fractionation correction. The background for all the samples in analytical procedures was Rb and Sr < 1*ng* and Sm and Nd < 0.1ng. Analytical precision is < 0.010% (2σ, same below) for $^{87}Rb/^{85}Rb$, < 0.0020% for $^{87}Sr/^{86}Sr$ without diluent, < 0.010% for $^{87}Sr/^{86}Sr$ with ^{84}Sr diluent, <0.0020% for $^{143}Nd/^{144}Nd$, < 0.010% for $^{150}Nd/^{144}Nd$ and < 0.010% for $^{147}Sm/^{152}Sm$. During the course of this study, Repeated measurements of standards NBS987 and La Jolla yielded the $^{87}Sr/^{86}Sr$ ratio of 0.710232±0.000007 (2σ, n = 8) and $^{143}Nd/^{144}Nd$ ratio of 0.511842±0.00006 (2σ, n = 16), respectively, which are consistent with the suggested values within the error range.

4. Whole-Rock Geochemistry

4.1. Major Elements Analyses

In the SiO_2 vs. K_2O+Na_2O (Figure 3a) and Nb/Y vs. Zr/TiO_2 (Figure 3b) Diagrams, all sample data fall in the fields of basalt, basaltic andesite, andesite, dacite and rhyolite. The basalts have SiO_2 contents of 48.78~52.14 wt.% (mean=50.2 wt.%), TiO_2 of 0.86~0.97 wt.% (mean=2.05 wt.%), which are significantly different from intraplate basalts (>2 wt.%), mid-ocean ridge basalts (1.5 wt.%), but similar to island arc basalts (0.84 wt.%) [26]. Their K_2O and K_2O+Na_2O contents range between 0.98 wt.~3.93 wt.% (mean=2.05 wt.%), 2.95~8.19 wt.% (mean=5.59 wt.%), respectively, with K_2O/Na_2O ratios of 0.5~1.4 (mean=0.75). In contrast, the acidic volcanic rocks are characterized by high SiO_2 (64.55~79.25 wt.%, mean=74.55 wt.%), K_2O (1.03~3.71 wt.%, mean=2.16 wt.%) and K_2O+Na_2O (4.28~7.61 wt.%, mean=6.09 wt.%), moderate Al_2O_3 (11.71~17.76 wt.%, mean=14.20 wt.%), low TiO_2 (0.09~0.51 wt.%, mean=0.21 wt.%), and K_2O/Na_2O ratios varies greatly, ranging from 0.18 to 6.31 (mean=1.69), but mostly less than 0.5. Their TiO_2 contents are close to the acidic volcanic rocks in the Andean continental margin (0.18 wt.%), and Al_2O_3 contents are similar to the rhyolite in the continental margin of the western United States [26]. A/CNK ratios are 1.04~2.56, (mean=1.47) and AR values are usually less than 2.5, indicating that the magma was the product of high degrees of partial melting [27], and during the process of evolution, more shell-derived materials were mixed in. The $Mg^{\#}$ values of the samples range from 47 to 68 (mean=57.9) except for sample SD29 (15). In the SiO_2 vs. K_2O diagram (Figure 3c), the main body is distributed in the low-k calc-alkaline rock field, and some of them fall in the fields of high potassium and potassium basalt. The AFM diagram (Figure 3d) shows a typical calc-alkaline sequence evolution trend, indicating the characteristics of volcanic rocks in the subduction zone. In Figure 4, the content of SiO_2 is negatively correlated with the contents of Fe_2O_3, Al_2O_3, MgO, CaO, TiO_2, P_2O_5 and MnO, and positively correlated with total alkali (K_2O+Na_2O). Their linear relationship is obvious, suggesting that they may have derived from a unified provenance and revealing that pyroxene, hornblende, feldspar, apatite and titanium-rich minerals (such as ilmenite) crystallized and separated during the magmatic evolution.

Table 1. *Major (wt.%) and trace (ppm) elements compositions of Carboniferous volcanic rocks in Eastern Junggar.*

Samples	SD04	SD05	SD06	SD11	SD26	SB29	SD21	SD14	SD17	SD29	SB2	SB16	SB33	SB40
	Basalt	Basalt	Basalt	Basalt	Basalt	Basalt	Dacite	Rhyolite	Rhyolite	Rhyolite	Rhyolite	Rhyolite	Rhyolite	Rhyolite
SiO_2	49.18	48.93	51.94	50.21	48.78	52.14	64.55	74.65	73.16	78.65	79.25	74.12	78.21	73.84
TiO_2	0.88	0.86	0.89	0.89	0.97	0.89	0.51	0.18	0.18	0.09	0.15	0.17	0.15	0.21
Al_2O_3	14.50	14.30	15.32	16.45	12.00	15.62	17.76	13.81	13.72	11.71	12.29	13.76	13.24	14.37
Fe_2O_3	3.50	2.94	2.13	2.37	2.21	1.31	2.30	0.32	0.68	0.71	0.73	0.52	0.62	0.56
FeO	6.19	6.51	6.14	6.27	7.25	6.81	1.35	0.33	0.50	0.15	0.16	0.25	0.18	0.15
MnO	0.18	0.28	0.24	0.19	0.25	0.24	0.05	0.03	0.04	0.02	0.01	0.03	0.01	0.03
MgO	4.66	4.59	7.86	6.74	10.68	7.83	2.07	0.65	0.80	0.08	0.52	0.51	0.53	0.64
CaO	7.21	7.04	9.09	9.13	11.70	9.26	2.49	1.39	1.82	0.26	0.11	1.72	0.10	1.57
Na_2O	4.27	3.28	2.66	1.97	1.87	2.55	5.65	5.19	5.21	4.12	0.70	4.99	0.59	5.06
K_2O	3.93	3.42	1.51	0.98	1.67	1.48	1.03	1.31	1.25	3.50	3.57	1.45	3.71	1.43
P_2O_5	0.49	0.48	0.28	0.32	0.32	0.29	0.15	0.07	0.08	0.04	0.03	0.08	0.05	0.09

Table 1. *Continued.*

Samples	SD04	SD05	SD06	SD11	SD26	SB29	SD21	SD14	SD17	SD29	SB2	SB16	SB33	SB40
	Basalt	Basalt	Basalt	Basalt	Basalt	Basalt	Dacite	Rhyolite	Rhyolite	Rhyolite	Rhyolite	Rhyolite	Rhyolite	Rhyolite
LOI	4.93	7.29	1.81	4.48	2.02	1.46	1.88	1.98	2.39	0.61	2.39	2.28	2.38	2.05
Total	99.91	99.91	99.88	99.99	99.72	99.86	99.80	99.90	99.83	99.92	99.92	99.89	99.75	99.99
$Mg^{\#}$	47.35	47.46	63.72	59.07	67.56	63.82	52.13	65.37	56.40	15.31	53.58	55.94	56.28	64.04
Cs	3.24	1.94	11.22	5.98	5.40	11.25	5.86	2.74	2.64	1.65	3.68	2.92	1.73	3.15
Rb	114	94	124	53	66	122	46	102	92	91	139	106	123	99
Sr	690	462	431	412	490	437	506	111	95	117	40	95	45	114
Ba	449	334	170	257	585	133	235	139	106	418	470	122	589	142
Nb	5.6	5.4	2.3	2.9	2.1	2.3	4.2	7.0	6.8	5.6	5.5	7.3	8.3	6.5
Ta	0.42	0.41	0.18	0.29	0.16	0.17	0.31	0.68	0.65	0.87	0.62	0.72	0.87	0.61
Zr	88	102	52	62	39	53	86	150	144	91	88	147	112	150
Hf	2.59	2.86	1.55	1.77	1.34	1.65	2.63	5.54	5.39	3.47	3.56	5.59	4.22	5.51
Th	5.28	4.98	1.32	1.57	2.75	1.29	3.80	6.98	5.47	11.78	7.24	5.50	6.96	6.88
V	227	243	241	243	298	244	101	12	17	9	18	16	7	13
Cr	49.3	45.7	204.5	151.5	401.7	186.4	30.4	4.5	2	4.8	5.7	3.6	3.4	2.8
Co	33.2	33.9	28.4	37.6	32.7	28.1	15.9	0.5	1.0	0.7	0.3	0.7	0.2	0.6
Ni	21.6	19.3	72.5	68.1	82.9	72.3	21.8	3.2	4.3	2.7	1.4	3.6	1.3	2.4
Sc	28.0	26.4	35.8	29.0	53.2	33.3	12.7	2.9	3.3	2.9	4.2	3.4	3.9	3.0
U	1.90	1.98	1.02	0.68	0.57	0.77	0.65	1.60	2.07	5.76	3.29	1.45	5.37	1.98
Ti	4267	4671	4978	4695	5628	4982	3046	993	988	583	896	1029	858	1198
P	2237	2186	1245	1305	1486	1392	612	310	374	164	166	374	204	423
La	15.9	15.7	9.1	8.3	5.9	9.8	14.3	2.4	2.9	11.7	20.9	2.8	15.8	4.7
Ce	34.6	33.5	19.3	18.5	14.2	21.1	27.0	4.4	5.5	20.6	37.4	5.3	32.1	9.0
Pr	4.8	4.6	2.7	2.7	2.3	3.0	4.1	0.6	0.8	2.5	4.1	0.7	3.9	1.2
Nd	20.7	19.6	12.4	12.2	11.1	13.8	17.0	2.4	3.2	8.5	13.9	3.0	13.7	4.6
Sm	4.96	4.63	3.28	3.29	3.29	3.60	4.16	0.72	0.87	1.89	2.42	0.78	2.58	1.25
Eu	1.47	1.33	1.37	1.16	1.15	1.52	1.15	0.33	0.25	0.29	0.36	0.25	0.31	0.46
Gd	4.77	4.65	3.26	3.39	3.30	3.62	3.71	1.03	1.04	1.72	2.06	0.94	2.06	1.80
Tb	0.79	0.75	0.56	0.58	0.57	0.63	0.66	0.24	0.23	0.34	0.34	0.20	0.36	0.42
Dy	4.54	4.36	3.27	3.48	3.31	3.74	4.00	1.86	1.57	2.22	2.01	1.40	2.26	3.03
Ho	0.85	0.81	0.61	0.65	0.61	0.69	0.74	0.42	0.33	0.41	0.38	0.29	0.43	0.58
Er	2.49	2.40	1.76	1.87	1.69	2.01	2.19	1.40	1.04	1.27	1.20	0.96	1.44	1.84
Tm	0.41	0.39	0.28	0.31	0.27	0.34	0.36	0.25	0.20	0.22	0.21	0.18	0.26	0.32
Yb	2.60	2.57	1.79	1.93	1.73	2.14	2.37	1.80	1.31	1.55	1.50	1.31	1.75	2.12
Lu	0.45	0.43	0.32	0.33	0.28	0.36	0.40	0.32	0.26	0.26	0.27	0.25	0.30	0.36
Y	23.4	22.5	16.3	17.4	16.6	18.2	19.6	14.6	10.6	12.1	11.7	9.7	14.1	19.0
∑REE	99.32	95.57	59.99	58.56	49.57	66.41	82.16	18.11	19.43	53.46	87.06	18.38	77.35	31.61
$(La/Yb)_N$	4.38	4.38	3.63	3.07	2.45	3.29	4.32	0.95	1.56	5.42	9.98	1.55	6.49	1.59
Eu/Eu^*	0.91	0.87	1.27	1.05	1.06	1.28	0.87	1.18	0.80	0.48	0.48	0.88	0.40	0.94
Ce/Ce^*	0.96	0.96	0.94	0.96	0.95	0.94	0.85	0.88	0.88	0.89	0.93	0.87	0.97	0.91

LOI = loss on ignition, $Mg^{\#}=100\times Mg^{2+} / (Mg^{2+} + Fe^{2+})$, $(La/Nb)_N$ are the chondrite-normalized values from [27].

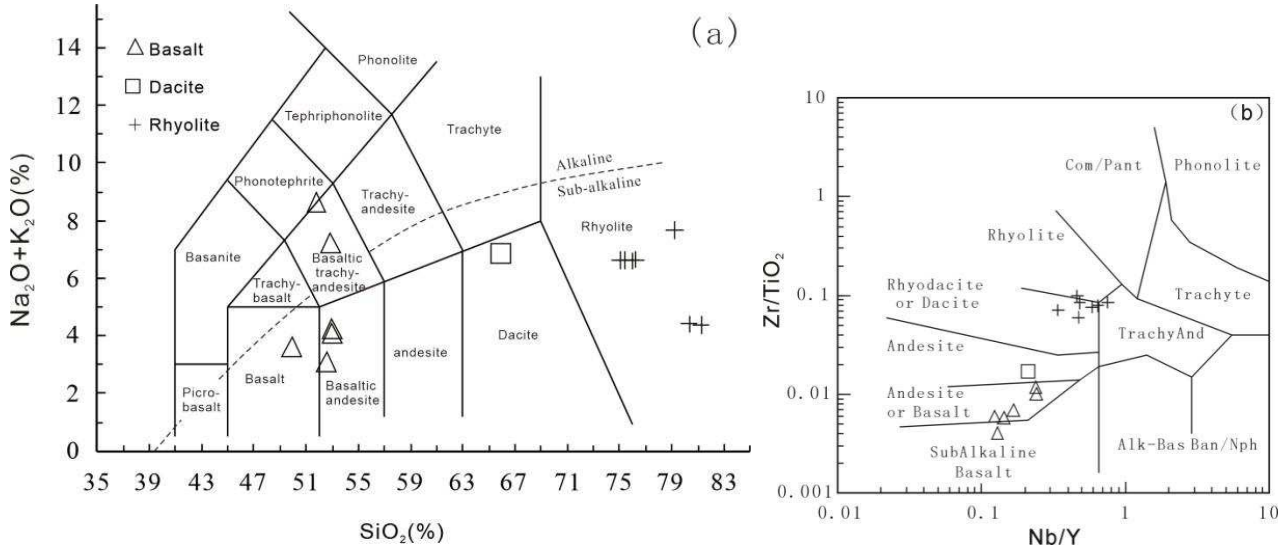

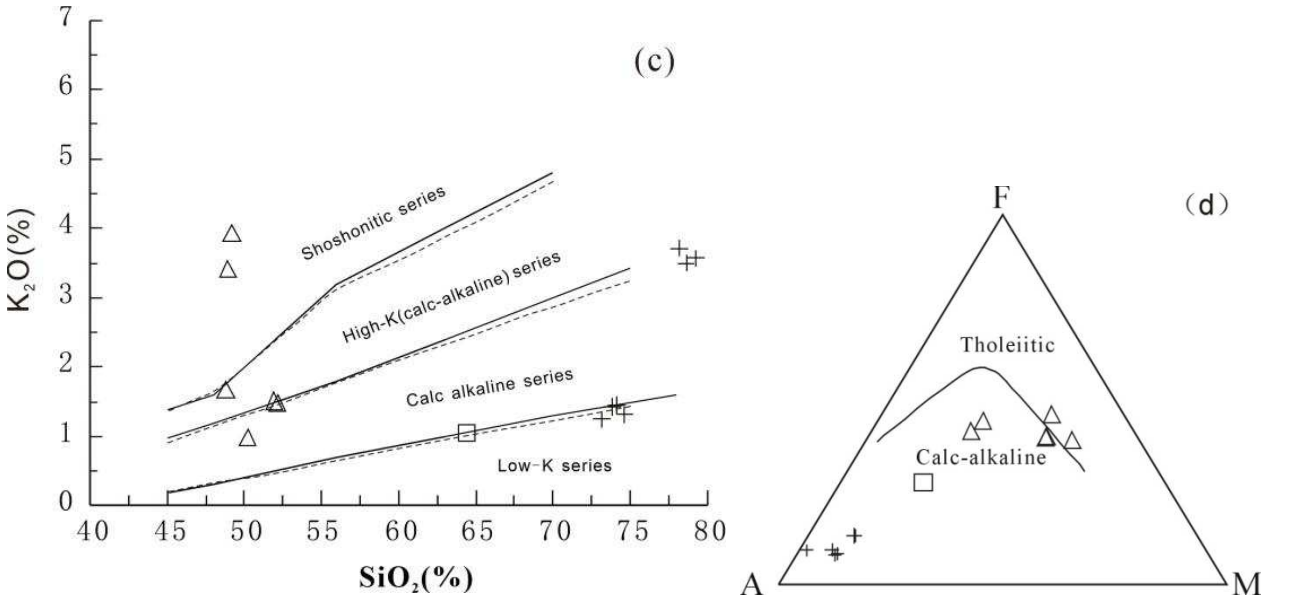

Figure 3. *SiO_2 vs. K_2O+Na_2O (after [28]), Nb/Y vs. Zr/TiO_2 (after [29]), SiO_2 vs. K_2O (after [30]) and AFM (after [31]) diagrams for the volcanic rocks from Kalamaili.*

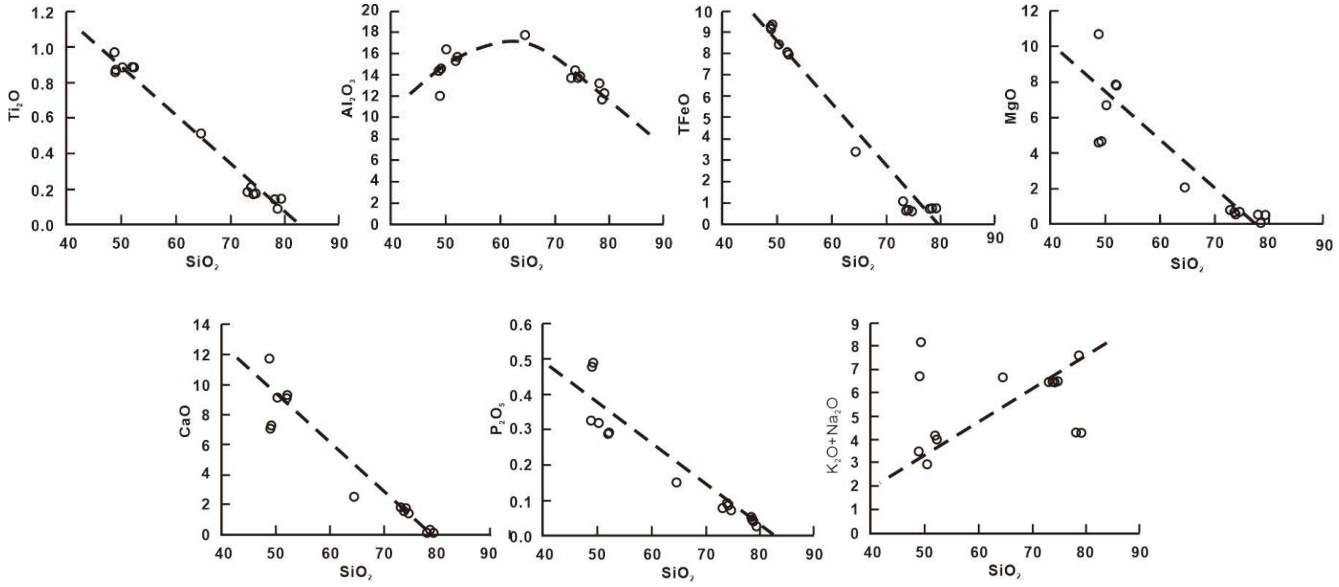

Figure 4. *Major oxide vs. SiO_2 variability diagrams for the volcanic rocks from Kalamaili.*

4.2. Trace Element Analyses

Trace elements of all samples are closely related to SiO_2 content and show regular changes. V, Cr, Co, Ni, Li, Sc, U, Ti and P are negatively correlated with SiO_2 content, Nb, Zr, Th and Hf are positively correlated with SiO_2 content, while Rb, Sr, Ba and Ga show little change. The contents of Cr, Co, Ni, and V in basalts are generally low, followed by 45.7~204.5 ppm (mean=173.18 ppm), 28.1~33.9 ppm (mean=32.30 ppm), 19.3~82.9 ppm (mean=56.12 ppm), 227~298 ppm (mean=249.3 ppm), and decreased with the decrease of MgO contents. The results show that the magma has undergone a significant crystallization separation of clinopyroxene in the magma chamber or during its ascent. This can be confirmed by field and microscopic observations of clinopyroxene phenocrysts prevalent in basalts. In the standardization partition diagram of trace element N-MORB (Figure 5), the volcanic samples show enrichment of large ion lithophile elements Sr, K, Rb, Ba, Th and depletion of high field strength elements Ta, Nb, Ti, which may be related to the mixing of some crust source materials in the magma origins. The trace element spider patterns (Figure 5) show a right-dipping, belonging to the enrichment type of strongly incompatible elements, with typical characteristics of continental arc calc-alkaline volcanic rocks [32]. Their N-MORB-normalized trace elements spider patterns are similar, suggesting that they may be driven from analogous magma sources and the result of homologous magmatic evolution. In addition, the acidic volcanic rocks, compared with the basalts, are poor in Sr, Ce, P and Ti, but rich in Rb, Ta, Th and Nb, indicating the crystallization separation of

plagioclase, apatite and titanium-rich minerals in the late magmatic evolution. Moreover, the significant Rb and Th peaks are considered the characteristics of acidic volcanic rocks in subduction zones [33].

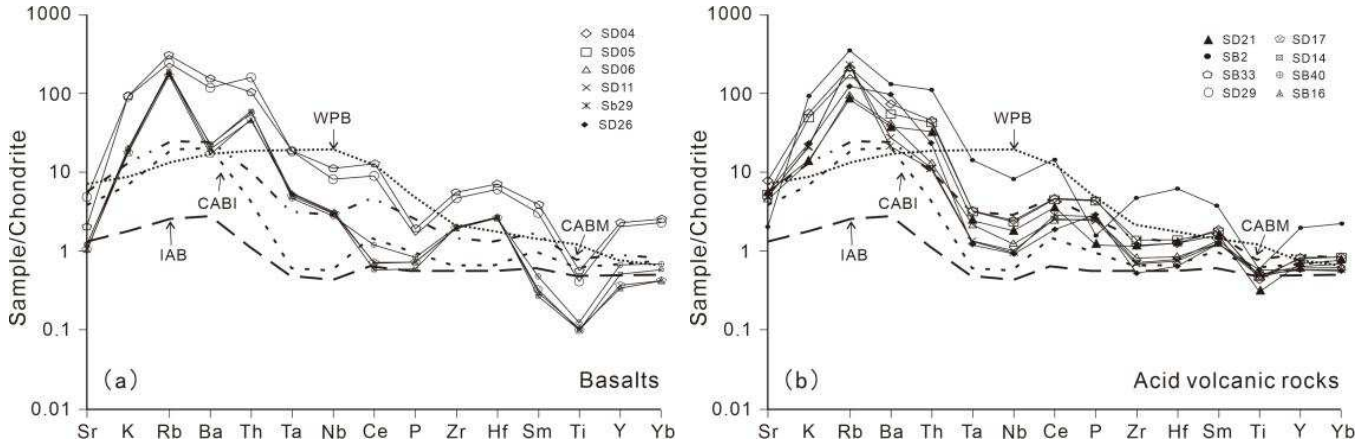

Figure 5. *N-MORB-normalized trace elements spider patterns diagrams for the volcanic rocks from Kalamaili. N-MORB-normalized values are from [27]; The data of WPB, CABM, CABI and IAB from [34, 35]. WPB: Within Plate Basalts; CABM: Continental Arc Calc Alkaline Basalts; CABI: Island Arc Calc Alkaline Basalts; IAB: Island Arc Tholeiites.*

4.3. Rare Earth Elements Analyses

The basalts have ΣREE contents of 49.57~99.32 ppm (mean=71.57 ppm), LREE/HREE ratios of 3.32~4.88 (mean=4.10), $(La/Yb)_N$ ratios of 2.45 to 4.38 (mean=3.53), $(La/Sm)_N$ ratios of 1.16~2.18 (mean=1.76), $(Gd/Yb)_N$ ratios of 1.40~1.58 (mean=1.12), Eu/Eu^* of 0.87~1.28 (mean=1.04), Ce/Ce^* of 0.94~0.96 (mean=0.92) (Table 1). In the chondrite-normalized REE patterns (Figure 6a), the basalts display enrichment in LREEs and depletion in HREEs with slight negative Eu anomalies, which is obviously different from the N-MORB and OIB volcanic rocks and similar to those of island arc calc-alkaline volcanic rocks. The REE contents of acid volcanic rocks are relatively low and variable, ranging from 18.11 ppm to 87.06 ppm (mean=71.57 ppm), with LREE/HREE ratios of 1.48~9.91 (mean=4.51), $(La/Yb)_N$ ratios of 0.95~9.98 (mean=3.98), $(Gd/Yb)_N$ ratios of 1.40~1.58, $(La/Sm)_N$ ratios of 2.13~5.57 (mean=3.09), $(Gd/Yb)_N$ ratios of 0.47~1.29 (mean=0.84), Eu/Eu^* of 0.40~1.18 (mean=0.75), and slight negative Ce anomaly. Figure 6b shows that the REE patterns of the acid volcanic rocks are significantly distinct from the basalts and can be subdivided into two types: (1) One is relatively slight right-dipping and parallel to those of basalts and andesites, with relatively lower ΣREE contents, weak-broad U-shaped negative Eu anomaly and no obviously negative or weakly positive Eu anomaly. The REE patterns are similar to the distribution curves of the metasomatic harzburgite xenoliths, suggesting that its genesis may be related to mantle rocks subject to LREE-enriched fluids or partially molten magma accounting for the anomalous LREE deficit [32]; (2) Another is more steeply right-dipping, with strongly LREE enriched and significant V-shaped negative Eu anomalies, which is similar to that of the strongly differentiated crust-mantle mixed granite, indicating that the magma source area may have been subjected to more intense crustal mixing.

5. Sr-Nd Isotope Geochemistry and Sm-Nd Isochronal Ages

5.1. Sr-Nd Isotope Analyses

The Sr-Nd isotopic compositions are given in Table 2. The $^{87}Sr/^{86}Sr$ and $^{143}Nd/^{144}Nd$ ratios of the analyzed samples are 0.706025 ~ 0.756232 and 0.512645 ~ 0.513368, respectively. The initial Sr-Nd isotopic ratios were calculated using the age of 320 Ma, based on the development of middle-late carboniferous animal and plant fossils in this suite of volcanic rocks. The results are presented that the volcanic rocks have initial $^{87}Sr/^{86}Sr$ ratios of 0.70385~0.71312, $^{143}Nd/^{144}Nd$ ratios of 0.512378~0.512998 and positive $\varepsilon_{Nd}(t)$ values of 3.0~6.2 except for sample SD14 (15.1) and sample SD16 (8.2), which are obviously different from crust-derived volcanic rocks and show the characteristics of originating from depleted mantle. However, the lower ε_{Nd} (t) values may exhibit that crust-mantle interactions have occurred in the process of parent magma evolution, because the island-arc volcanic rocks derived from the melting of mantle wedge often have such characteristics [36]. The Sm/Nd-ε_{Nd} (t) diagram (Figure 7a) shows that the Sm/Nd ratios are relatively concentrated, indicating that the volcanic rocks in the Batamayineishan Formation were affected by crystallization differentiation and partial melting during their formation process [37].

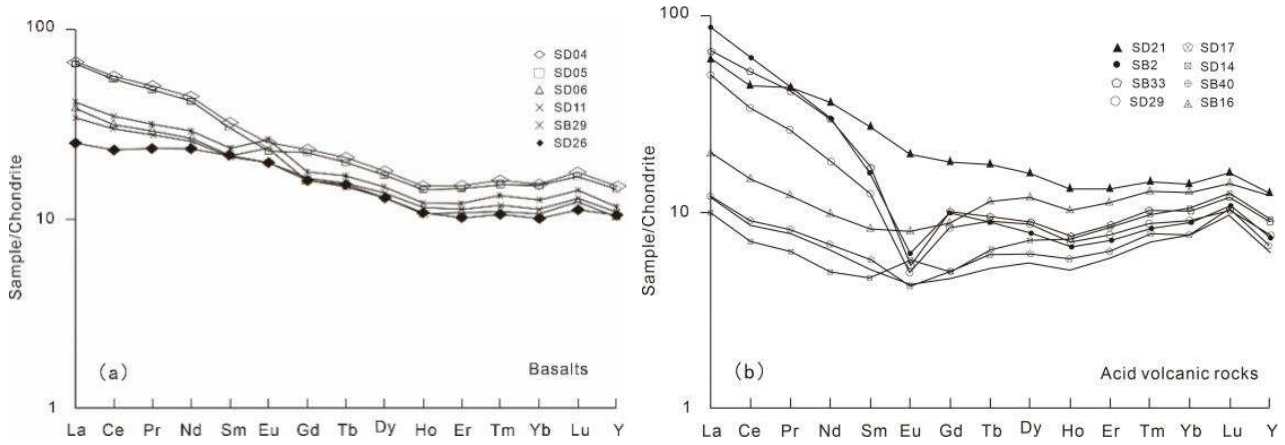

Figure 6. *Chondrite-normalized REE patterns diagrams for the volcanic rocks from Kalamaili. Chondriite-normalized values are from [27].*

Table 2. *Sr-Nd isotopic compositions of Carboniferous volcanic rocks in Eastern Junggar.*

Sample	Rb (ppm)	Sr (ppm)	$\frac{^{87}Rb}{^{86}Sr}$	$\frac{^{87}Sr}{^{86}Sr}$ (±2δ)	Sm (ppm)	Nd (ppm)	$\frac{^{147}Sm}{^{144}Nd}$	$\frac{^{143}Nd}{^{144}Nd}$ (±2δ)	$I_{Nd}(t)$	$I_{Sr}(t)$	εNd (*t*)	$f_{Sm/Nd}$	T_{2DM}(Ga)
SD04*					5.24	20.59	0.1538	0.512736±2	0.512414		3.7	-0.22	0.78
SD11*					3.28	11.70	0.1694	0.512769±5	0.512414		3.7	-0.14	0.78
SD31*					4.41	16.74	0.1593	0.512747±3	0.512413		3.7	-0.19	0.78
SD51*					4.75	19.02	0.1510	0.51273±2	0.512414		3.7	-0.23	0.78
SD52*					5.17	20.67	0.1513	0.512731±1	0.512414		3.7	-0.23	0.78
SB19*					4.89	19.50	0.1517	0.512732±7	0.512414		3.7	-0.23	0.78
SB29*					3.30	11.61	0.1719	0.512774±2	0.512414		3.7	-0.13	0.78
SB77*					3.59	12.58	0.1725	0.512775±3	0.512414		3.7	-0.12	0.78
SD14	98.8	132.9	2.1504	0.716884±5	1.45	4.96	0.1764	0.513368±15	0.512999	0.707100	15.1	-0.10	
SD17	94.3	103.2	2.6449	0.717763±3	0.89	3.15	0.1704	0.512771±2	0.512414	0.705729	3.7	-0.13	0.78
SD21	45.1	579.7	0.2250	0.706025±3	4.83	19.74	0.1480	0.512688±6	0.512378	0.705001	3.0	-0.25	0.84
SD29	87.7	123.1	2.0606	0.715408±5	2.34	10.20	0.1389	0.512673±4	0.512382	0.706032	3.1	-0.29	0.83
SB02	142.1	39.7	10.3702	0.756232±4	2.57	14.05	0.1105	0.512718±7	0.512487	0.709047	5.1	-0.44	0.67
SB16	105.9	104.1	2.9438	0.719496±5	0.85	3.08	0.1668	0.512995±21	0.512646	0.706102	8.2	-0.15	0.41
SB33	120.3	48.4	7.1881	0.745857±3	2.64	13.77	0.1157	0.512645±4	0.512403	0.713151	3.5	-0.41	0.80
SB40	105.5	111.6	2.7341	0.716301±5	0.77	2.52	0.1836	0.512926±12	0.512542	0.703861	6.2	-0.07	0.59

*are for Basalts.

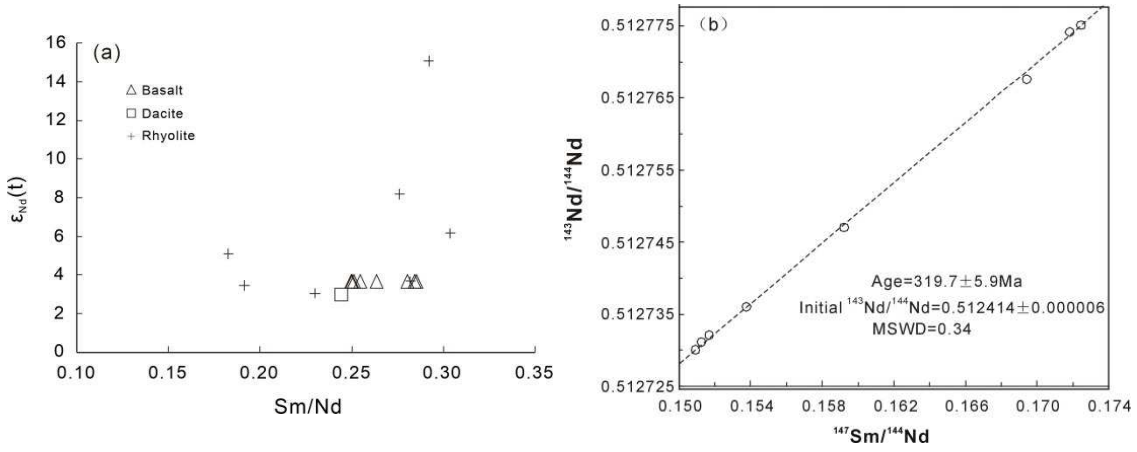

Figure 7. *Sm/Nd vsεNd (t=320Ma) (after [38]) and isochron age of Sm-Nd isotopic systematics diagrams for the volcanic rocks from Kalamaili.*

5.2. Sm-Nd isochron Age Analyses

The $^{147}Sm/^{144}Nd$ ratios of basalts are 0.1510 ~ 0.1725, the ratios of $^{143}Nd/^{144}Nd$ are 0.512730 ~ 0.512775, the initial $^{143}Nd/^{144}Nd$ ratios are 0.512413 ~ 0.512414, and all the values of ε_{Nd} (t) are 3.7. The values of each parameter are relatively uniform, showing the characteristics of the evolution of homologous magma and better sealing conditions. In contrast, the parameters of acid volcanic rocks vary widely from 0.1105 to 0.1836, 0.512645 to 0.513368,

0.512531 to 0.512998, and 3.0 to 15.1, respectively, which are obviously distinct from those of basalts and indicates that their origin shows the characteristics of multiple sources. Therefore, it is reasonable to select eight basalt samples in Table 2 for Sm-Nd isochron age calculation. The results show that eight samples showed good linear correlation (Figure 7b), and the isochronal age of the basalts is (319.7±5.9) Ma, initial $^{143}Nd/^{144}Nd$ ratio is 0.512414± 0.000006 (MSWD = 0.34), which is consistent with the age evidence from animal and plant fossils in the Batamayineishan Formation. In addition, these basalt samples have higher $^{147}Sm/^{144}Nd$ ratios (>0.14) and $f_{Sm/Nd}$ ratios (-0.12 ~ -0.23). Therefore, the two-stage model age calculation method was adopted to calculate the T_{2DM} value of volcanic rocks. The result is 0.78Ga and far older than its isochron age (319.7±5.9) Ma, similar to the results of Long Xiaoping et al. [15]. Combined with its smaller positive $\varepsilon_{Nd}(t)$ values of the samples, it may indicate that crust-mantle interaction and Sm-Nd isotope homogenization had occurred in the deep magma chamber before (319.7±5.9) Ma.

6. Discussion

6.1. Formation Age

There are still a few different views on the age of formation of the Batamayineishan volcanic rocks. The previous studies suggested that they were formed in late Early Carboniferous to early Late Carboniferous based on the fossils of animals and plants in the Batamayineishan Formation and their contact with the upper and lower strata[1][2]. In recent years, many geochronological studies for them have been performed. Tan et al. [4] obtained zircons weighted mean U-Pb age of (350.0±6.3) Ma for the trachyandesites in Kalamaili, with the conodont fossils of early-late carboniferous in Shuangjingzi Formation and Shiqiantan Formation overlying Batamayineishan volcanic rocks, and identified that they were formed in the Early Carboniferous. Zhang et al. [39] yielded zircons weighted mean U-Pb age of (275.6±2.8) Ma for the rhyolites in Zhaheba and considered that they erupted in the Early Permian. The study results of Su et al. [6, 7] and Yang et al. [40] are complicated and the obtained zircons U-Pb ages for the basalts, trachytes and rhyolites may be divided into multiple groups, ranging from 500Ma~300Ma, and they believed that (300.4±1.3) Ma and (318.7±4.2) Ma represented the formation age of Batamayineishan volcanic rocks. However, the cathodoluminescence images of the zircons from Tan et al. [4] show that some of the zircons have poorer grain shapes or rounded shapes, exhibiting obvious characteristics of inherited zircons. Moreover, the latest studies indicate that the Batamayineishan volcanic rocks have significant characteristics of mixed crust-mantle sources [10, 11, 13-15], and there are plenty of captured early magmatic crystallization zircons in the Carboniferous volcanic rocks, and the residual oceanic crust of Junggar ocean basin was survived in Eastern Junggar since Devonian [1, 40, 41]. In addition, it is easy to capture zircons in surrounding rocks along the way of magma upward intrusion because of the rapid ascending and cooling rate of volcanic magma. Therefore, we argue that the volcanic eruption around 320Ma is likely to involve some materials of earlier magmatic events, and the (350.0±6.3) Ma obtained by Tan et al. [4] probably represents the mixed age of this event. Samples for zircon U–Pb dating were collected from Zhaheba and Ludong-Wucaiwan in Eastern Jugger by Zhang et al. [39] and Su et al. [6, 7], respectively, where the volcanic rocks and intrusive dikes of Early Permian or later are widely exposed [4, 16, 25, 42, 43]. Thus, it remains to be further studied for the zircons in Batamayineishan volcanic rocks whether they have been influenced by this extensive and intense magmatism.

The samples in this study were collected from Songkarsu in Kalameli where the volcanic rocks are exposed widely and can be connected with the Batamayineishan Formation in Batamayinishan, representing the volcanic rocks of the Batamayineishan formation. The analysis results show that the Sm/Nd and $^{147}Sm/^{144}Nd$ ratios of samples vary greatly, $^{143}Nd/^{144}Nd$ ratios vary gently and $\varepsilon_{Nd}(t)$ values range between 3.66 and 3.67. These features are remarkably distinct from the crust-derived volcanic rocks and display the characteristics of the volcanic rocks of depleted mantle origin. Although the lower $\varepsilon_{Nd}(t)$ values of samples may reveal that the crust-mantle interaction has occurred before this volcanic diagenesis, the characteristics of their similar $\varepsilon_{Nd}(t)$, T_{2DM} values and major elements, trace elements and rare earth elements compositions imply that the crust-mantle interaction was not generated by the crustal contamination during the process of magma ascent, and it is more likely to the origin of crust-mantle magmatic mixing thoroughly in volcanic magma source. Under the condition, the Sm-Nd isotopic system of the mixed magmas has undergone complete homogenization and always maintained good sealing conditions. Consequently, eight basalt samples for Sm-Nd isochronal dating are qualified. These samples yield an Sm-Nd isochron age of (319.7 5.9) Ma (Figure 7b), which is not only consistent with the tectonic setting of Eastern Junggar, but also with the evidence from most animal and plant fossils in Batamayneshan Formation, representing the age of Batamayneshan volcanic rocks. Meanwhile, this result has been supported by other studies [7, 8, 10, 11, 44].

6.2. Tectonic Setting

The volcanic rocks in Songkarsu are characterized by basalt, andesite, dacite and rhyolite, with amounts of tuffs and volcanic breccias. They contain relatively high K_2O and ALK contents, medium Al_2O_3 contents and low TiO_2 contents. They are ascribed to high potassium calc-alkaline volcanic rocks and their major elements show consistent geochemical evolution trends with increasing SiO_2, reflecting that they differ from the intra-oceanic arc volcanic rocks

1 Xinjiang Geological Bureau.1966. Kupu (L-466-XXV) 1:200 000 regional geological survey report.

2Xinjiang Geological Bureau.1980. Laojunmiao (L-46-XXV) 1:200 000 regional geological survey report.

mainly composed of medium-k calc-alkaline basalts and andesites, but similar to the typical continental arc or active continental margin arc volcanic rocks [26].

Strongly incompatible elements are generally less active and relatively stable in post-magmatic alteration, which are favorable indicators for studying on the material source and tectonic setting of volcanic rocks. The basalt samples have Nb contents of 2.1~5.6 ppm (mean=3.4 ppm), Ta contents of 0.16~0.42 ppm (mean=0.27 ppm), with varying slightly, approximate to the contents of oceanic ridge tholeiites (4.6 ppm, 0.29 ppm, respectively) and volcanic arc basalts (1.7~8.4 ppm, 0.10~0.33 ppm, respectively) [27, 32]. In contrast, the acid volcanic samples have Nb and Ta contents of 4.2~8.3 ppm (mean=6.4 ppm) and 0.31~0.87 ppm (mean=0.67 ppm), respectively, which are significantly lower than typical intraplate basalts (>10 ppm, >>1.0 ppm, respectively) [32], but similar to those of continental crust (8.0 ppm, 0.7 ppm, respectively) [45], suggesting that they may contain more crust-derived materials. In addition, all samples are enriched LILEs (Th, Rb, Ba and K), depleted HFSEs (Na, Ta and Ti) and $(La/Yb)_N$ >>1, which are different from oceanic ridge basalts and mostly considered the signatures of subduction zone basalts. However, many studies have proved that these phenomena could also occur in extension settings of post-collision, continental rifts and back-arc basins related to crustal contamination [26, 45-48].

In general, the addition of crustal materials will lead to the content increase of LILEs (such as Rb, Ba, Th, etc.) and decrease of HFSEs (Na, Ta, Ti, etc.), as well as the increase and decrease of the corresponding ratios. Extremely high $(Th/Nb)_{PM}$ (>>1) [49] and La/Nb (>1) [50] ratios are considered to be two important parameters to characterize crustal contamination, with indicative effects almost similar to those of isotopes. The basalt samples have $(Th/Nb)_{PM}$ ratios 4.54~10.81, Nb/La ratios 0.23~0.36, La/Ba ratios 0.01~0.07, Ba/Nb ratios mostly less than 100, Ta/Nb ratios 0.07~0.10 close to 0.10 from the upper crust. These ratios in acid volcanic samples are 6.28~17.65, 0.26~2.94, 0.02~0.06, 15.50~83.36, 0.07~0.16 [51, 52], respectively. This indicates that the formation of Batamayneshan volcanic rocks has experienced the contamination of crustal materials in variable degrees. The elements of Ti, Zr and Y are relatively stable and may be used to identify the tectonic environment of volcanic rocks formed by the contamination of crust or lithospheric mantle materials [47, 53]. Xia et al. [47] suggested that the volcanic rocks in intraplate settings commonly are characterized by TiO_2>1%, Zr>70 ppm, Zr/Y>4 and Ti/Y>400, whereas those in convergent plate margin settings are TiO_2<1%, Zr<130 ppm, Zr/Y<3.5 and Ti/Y<500. The contents of TiO_2 in studied volcanic rocks are generally lower than 1.0. Among them, the basalt samples have Zr contents of 39 ~102 ppm, Zr/Y ratios of 2.37~4.54, Ti/Y ratios of 182.58~339.87, La/Nb ratios of 2.76~4.36. Correspondingly, the acid volcanic samples have Zr ranging from 86 ppm to 150 ppm, Zr/Y ranging from 4.40 to 15.08, and Ti/Y ranging from 50 to 100. These features indicate the Batamayneshan volcanic rocks are similar to continental arc volcanic rocks [54], inconsistent with those in an intraplate setting. In addition, high incompatible elements contents, εNd(t) values, low HFSEs contents as well as low initial $^{87}Sr/^{86}Sr$ and $^{143}Nd/^{144}Nd$ ratios also support that they are formed in a continental arc setting.

Many studies have been carried out for Batamayneshan volcanic rocks in Eastern Junggar. The results display that they are similar characteristics in their petrology and geochemistry, but some discussions on the diagenetic tectonic setting of volcanic rocks persist. Most geologists suggested that they were formed in a post-collisional extensional setting [3, 6, 10] [12-14, 40], whereas the minority provided the proposal of volcanic arc setting genesis [15, 17, 55]. Indeed, the intraplate basalts undergone strong crustal contamination also have the characteristics of subduction zone volcanic rocks [47, 56]. However, the bimodal-type volcanic rocks are usually occurred in post-collisional extensional setting, accompanied by S-type granites and metamorphic rocks related to collisional orogeny and gabbro-diabase dikes in variable degrees, of which the basalts are mainly tholeiitic and alkaline and the acid volcanic rocks all occur including normal to alkaline [32, 56]. Based on the studies of previous and ourself on Batamayneshan volcanic rocks, the results present that their types are complex, including basalts, andesites, dacites and rhyolites, and clearly distinct from bimodal volcanic suites, as well as without corresponding gabbro-diabase dikes and intrusive and metamorphic rocks related to a collision. They are high-K calc-alkaline volcanic series, with the characteristics of relatively low Th/Ta ratios and initial $^{87}Sr/^{86}Sr$ and $^{143}Nd/^{144}Nd$ ratios, high εNd (t) values and depleted HFSEs, obviously inconsistent with the volcanic rocks formed in the post-collision extensional setting. Combined with the characteristics of voluminous and multi-staged eruptions for a long time of the Batamayneshan volcanic rocks in Eastern Junggar, we believe that they are impossibly formed in the stage of post-collisional initial extension.

As shown in the Zr vs. TiO_2 (Figure 8a) and Ti/100-Zr-3Y (Figure 8b) diagrams, the basalt samples fall within the island arc and mid-oceanic ridge basalts fields, and in the diagrams of 2Nb-Zr/4-Y (Figure 8c), Rb-Y+ Nb (Figure 8d) and 3Tb -Th -2Ta (Figure 8e), all samples plot in the volcanic arc rocks field. In contrast, it is more complex in the Zr-Zr/Y diagram (Figure 8f) that the basalts including from Karameri, Zaheba and Ludong-Wucaiwan in Eastern Junggar, all fall into the fields of island arc, mid-ocean ridge and intraplate basalts. Those of them in Zhaheba and Kalamaili are similar, mainly falling around the transitional field of the three tectonic settings mentioned above, whereas others in Ludong-Wucaiwan all plot in the intraplate basalts field. These features demonstrate that the Batamayneshan volcanic rocks were probably formed in a special transitional tectonic setting of the island arc, mid-ocean ridge or intraplate, not as any one of them. Dosso et al. [67] suggested that the volcanic rocks related to island arc and intraplate extension are commonly formed in the early stages of back-arc basin opening due to the influence of the mixing of two or more

end-member materials including mantle, subducted slab and crust, and then, as the extension developed and subduction weakened, the back-arc basin gradually reaches the mature stage to an oceanic basin with basalts presenting MORB characteristics. Based on the discussions above, the Batamayneshan volcanic rocks may have been formed in the back-arc basin. Additionally, they are consistent with the fields of typical back-arc basin basalts in the 3Tb -Th -2Ta (Figure 8e) and Zr-Zr/Y (Figure 8f) diagrams, confirming that they were formed in the back-arc basin. Furthermore, the regional geotectonic studies indicate the Paleo-Asian Ocean crust subduction southward under the Junggar-Tuha block along Zhaheba-Karamay during Devonian to Carboniferous has occurred [68-75], and Kalamaili-Darbut ophiolites represented Paleo-Asian Ocean crust have the characteristics of the back-arc basin [17, 76, 77] and SHRIMP zircon gains U-Pb ages of gabbro in them were (329.8±1.6) Ma [22] and (332±14) Ma [78]. These evidences not only give further support to the above result, but also reflect that the Batamayneshan volcanic rocks are likely to be the products of the back-arc basin represented by Kalamaili-Darbut ophiolites. However, minor volcanic rocks of them similar to those derived from the intraplate extension setting indicate that this back-arc basin remained an immature arc basin in the early stage of development, despite the initiation of oceanic ridge magmatism.

Back-arc basins are ordinarily a consequence of vast scale mantle materials upwelling and back-arc spreading caused by the continuous subduction of oceanic crust [32]. The occurrence of oceanic crust subduction in Eastern Junggar during late Early Carboniferous implied that the back-arc spreading was still in progress. Figure 8e and Figure 8f illustrate that the volcanic rocks in Zhaheba with the remarkable characteristics of the back-arc basin are perhaps associated with the arc basin expansion earlier due to their proximity to the subduction zone, and those in Ludong-Wucaiwan, far away from the subduction zone and close to the continental margins and the back-arc basin spreading latest, have been generated in the initial stage of back-arc basin spreading with Lithospheric thinning limited. Therefore, some geologists mistakenly believed that the Batamayneshan volcanic rocks were generated in the intraplate extensional setting. Whereas those in Kalamaili, located between Zhaheba and Ludong-Wucaiwan, demonstrate the characteristics of continental margin arc which are a transitional type of the above two types. In Eastern Junggar, the alkali granites with an age of 310-300Ma related to post-collision extension [79, 80] and Early Permian volcanic rocks with intracontinental rift characteristics [25, 42, 43] are outcropped widespreadly, indicating that the end of continent-continent convergent and Orogenic processes. In consequence, the final closure time of the Junggar ancient ocean basin should be earlier than 310 Ma, while its lower limit should be later than 320 Ma.

6.3. Petrogenesis and Magma Sources

The Batamayneshan volcanic rocks with relatively high $Mg^{\#}$ values (mostly >50), low contents of Cr, Co, Ni (especially in the acid volcanic samples) and positive $\varepsilon_{Nd}(t)$ values reveal that they are perhaps derived from depleted mantle sources, and the basalt rocks have undergone the slight-moderate fractional crystallization, while the acid volcanic rocks are more intense. Figure 9a shows a remarkably coherent linear correlation for the basalt samples, implying that they are similar in genesis, with the characteristics of comagmatic evolution. Whereas, the points of acid volcanic samples are scattered and no obvious linear correlation with the basalt samples, displaying that their genesis is more complex and has the characteristics derived from Multiple magma sources. Additionally, high $(Th/Nb)_{PM}$ ratios, low Nb/La, La/Ba and Ba/Nb ratios, Ta/Nb ratios similar to those in the crust and small positive $\varepsilon_{Nd}(t)$ values reveal that the Batamayneshan volcanic rocks have experienced variable degrees of crust-mantle interaction.

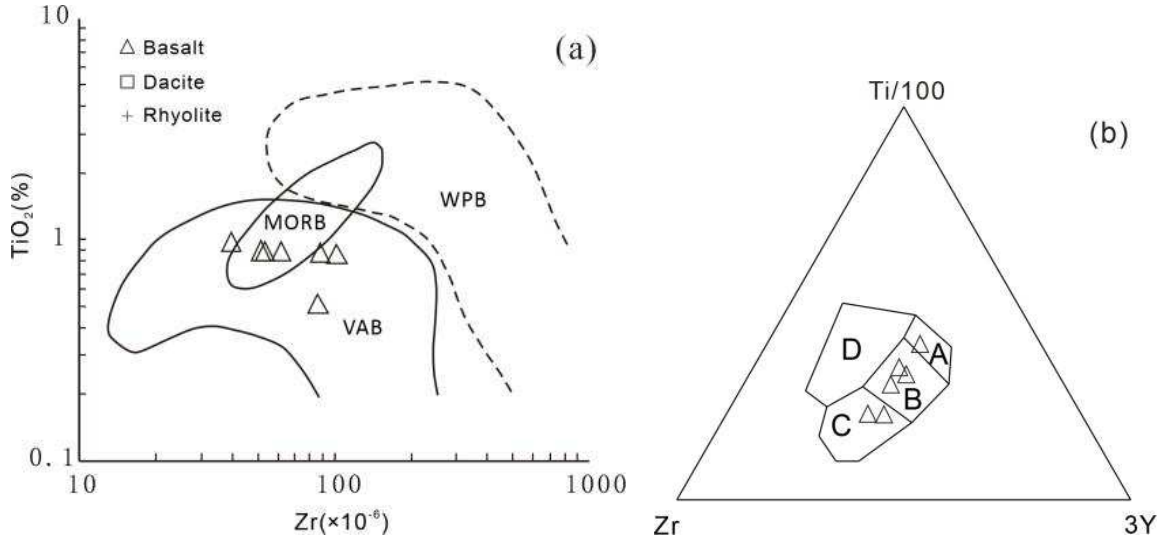

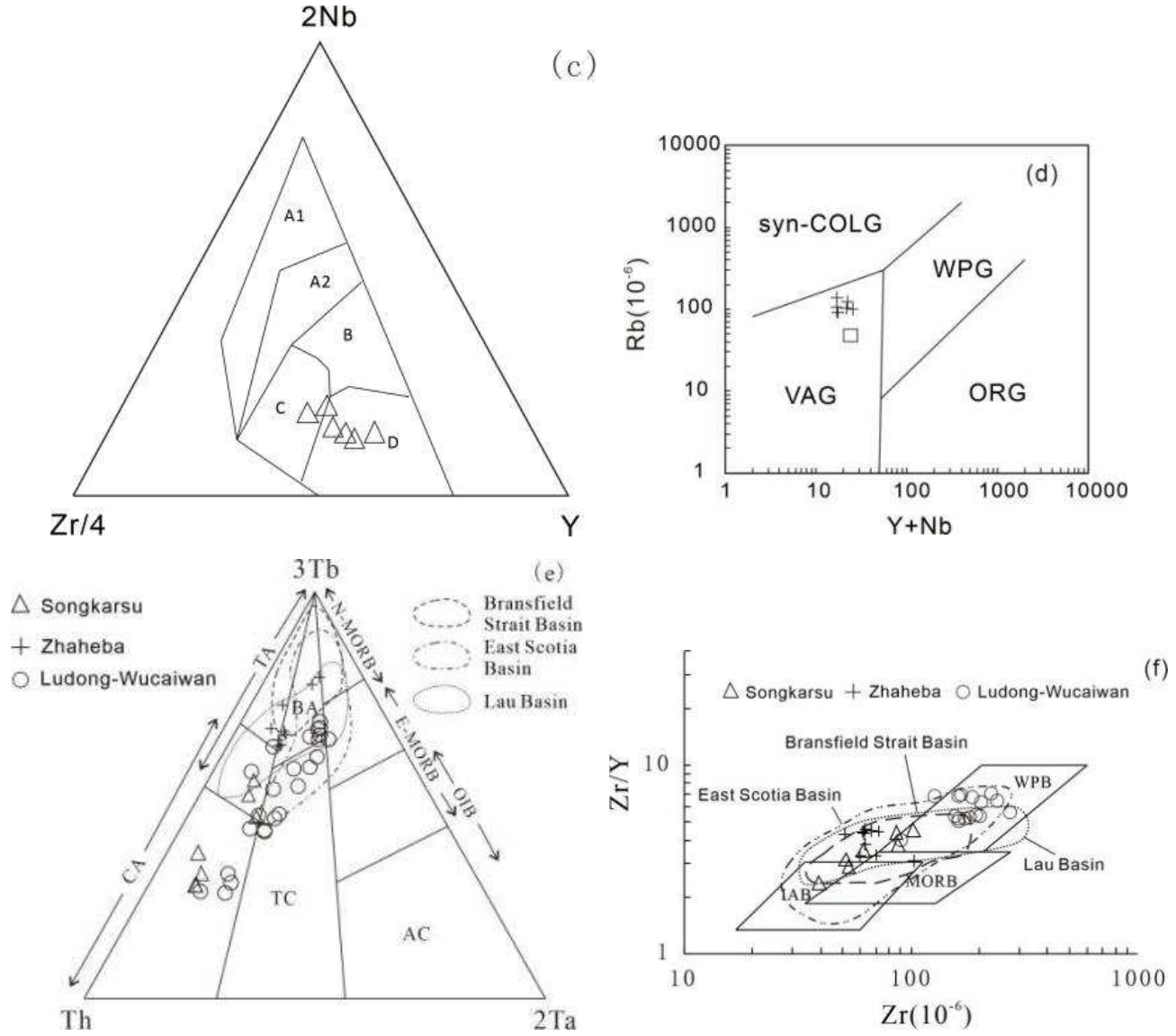

Figure 8. *Discrimination diagrams for tectonic settings for the volcanic rocks from Kalamaili. (a) after [57]. VAB: Island Arc Basalts; MORB: Mid-Ocean Ridge Basalts; WPB-Within Plate Basalts. (b) after [57]. A: Island Arc Tholeiites; B: Island Arc and Mid Ocean Ridge Basalts; C: Island Arc Calc Alkaline Basalts; D: Within Plate Basalts. (c) after [58]. A1+A2: Within Plate Alkaline Basalts; A2+C: Within Plate Tholeiites; B: E-type Mid-Ocean Ridge Basalts; D: Mid-Ocean Ridge Basalts; C+D: Volcanic Arc Basalts. (d) after [59]. VAG: Volcanic Arc Granites; syn-COLG: Syncollisional Granites; WPG: Within-Plate Granites; ORG: Oceanic Ridge Granites; (e) after [60]. N-MORB: N-type Mid-Ocean Ridge Basalts; E-MORB: E-type Mid Ocean Ridge Basalts; OIB: Island Basalts; TA: Island Arc Tholeiites; CA: Island Arc Calc Alkaline Basalts; BA: Back-Arc Basin Basalts; TC: Continental Arc Basalts; AC: Within Plate Alkaline Basalt. (f) after [61]. IAB: Island Arc Basalts; MORB: Mid-Ocean Ridge Basalts; WPB: Within Plate Basalts. Data for Ludong-Wucaiwan from [13, 14, 62]; Data for Zhaheba from [15]; Data for for Lau Basin from [63]; Data for Bransfield Strait Basin from [64]; Data for East Scotia Basin from [65, 66].*

Almost the same values of ε_{Nd} (t) and T_{2DM}, and similar compositions of major elements, trace elements and rare elements in the basalt samples reflect that they should be derived from the similar source areas. As discussed above, The Batamayneshan volcanic rocks are formed in a subduction-related back-arc basin, and their magmatic source areas, except for the dominant compositions of the depleted mantle, may contain the contributions of various components, including subducted ocean crust, continental crust and some fluids associated with them. In general, the subducted sediments have relatively high Th contents, low Ce/Th ratios (≈8) and Ba/Th ratios (≈111) [81]. Thus, the Batamayneshan basalts with Ce/Th ratios of 5.15~16.37 (mean=10.19), Ba/Th ratios of 67.11~212.92 (mean=126.85) and without clearly negative Ce anomalies indicate that their formation is impossibly involved the components of subducted sediment melt [82, 83]. Meanwhile, low Nb contents of 2.1~5.6 ppm (mean=3.4 ppm) is significantly different from basaltic volcanic rocks (Nb>7.0 ppm) produced by partial melting of subducted plates [84, 85]. Castillol et al. [86, 87] suggested that the Ba/La vs. La/Yb diagram has significant effects in identifying whether there is an addition of subducted oceanic crust and its overlying sediments during the formation processes of volcanic rocks. Figure 9b presents that most volcanic rock samples are far away from the fields of sediments and slab-derived melts, almost precluding the possibilities of that they are directly

derived by partial melting of the subducted slab or/and subducted sediments. However, the geochemical characteristics of volcanic arc rocks of them associated with crust-mantle mixing may well imply that their origins are related to the partial melting of the overlying mantle wedges caused by aqueous fluids from subducted sediments and/or subducted oceanic crust, and have been experienced slightly-moderately fractional crystallization during magma rising.

The mechanism of acid volcanic rocks commonly includes the following: (1) generated by the remelting of ancient crust, with remarkable negative $\varepsilon_{Nd}(t)$ values and high initial $^{87}Sr/^{86}Sr$ ratios; (2) generated by the remelting of young basaltic crust, with relatively low $Mg^{\#}$ values (<40), Sr/Y ratios (<10), small positive $\varepsilon_{Nd}(t)$ values and medium-high initial $^{87}Sr/^{86}Sr$ ratios; (3) generated by the crystallization differentiation of mantle-derived basic magmas, with high Sr/Y ratios (>10), positive $\varepsilon_{Nd}(t)$ values and low initial $^{87}Sr/^{86}Sr$ ratios; (4) generated by the mixing of crust-mantle magma, with the geochemical signatures of rhyolites produced by both the crystallization differentiation of the mantle-derived basic magmas and the remelting of crust, and their $\varepsilon_{Nd}(t)$ values are similar to those of associated basalts [7, 88-90]. The Batamayneshan acid volcanic rocks in Eastern Junggar with $\varepsilon_{Nd}(t)$ values of 3.0~15.1, initial $^{87}Sr/^{86}Sr$ ratios of 0.703861~0.713151 and the basement of Junggar Basin dominantly composed of the Paleozoic residual oceanic crust and island arc in different ages [7, 40, 89] suggest that they are impossibly formed by the remelting of ancient crust. Besides, high $Mg^{\#}$ values (<40) and low Sr/Y ratios (<10) of them indicate that they are distinctly different from the acid magmatic rocks generated by the crystallization differentiation of mantle-derived magmas and the partial melting of young crust, and more likely to be the result of crust-mantle magma interaction produced by the two sources mentioned above. Furthermore, other evidences for this view are as follows: (1) the acid volcanic samples are enriched in Zr, NB and Y, with relatively high $(Th/Nb)_{PM}$ ratios, Nb/La ratios and low La/Ba ratios, Ba/Nb ratios; (2) the $\varepsilon_{Nd}(t)$ values and initial ratios of $^{87}Sr/^{86}Sr$ and $^{143}Nd/^{144}Nd$ in acid volcanic rocks are not uniform and vary widely; (3) the T_{2DM} values of acid volcanic samples ranging from 0.4 to 0.8 are consistent with the intermediate-acid igneous rocks in different ages in Central Asian orogenic belt, as well as very close to the time of the large-scale expansion of Paleo-Asian Ocean recorded by the ophiolite and island arc complex in Eastern Junggar, suggesting that the formation of Batamayneshan acid volcanic rocks is associated with the subduction of ancient Asian ocean crust, and their magma sources area may be the subducted oceanic crust and its overlying mantle wedge [91]. As the above also shown, the crust-mantle magmatism of acidic volcanic rocks is obviously different from that of basalts, and the magma of them has been evolved in an open environment where the contamination of a few of young crust-derived materials plays an important role. However, the $\varepsilon_{Nd}(t)$ values of acid volcanic samples similar to the basalt rocks, and the distribution and good linear correlation of them in the Cr-Th diagram (Figure 9c) reflect the characteristics related to the crystallization differentiation of basaltic magma. On the basis of the above analysis, we can conclude that the formation of those acid volcanic rocks in the Batamayishan Formation should be formed by the interaction between crust-derived magma generated by partial melting of young crust and a small amount of mantle-derived magma, and they have been experienced the strong crystallization differentiation and crustal contamination of mantle basaltic magma in magmatic evolution.

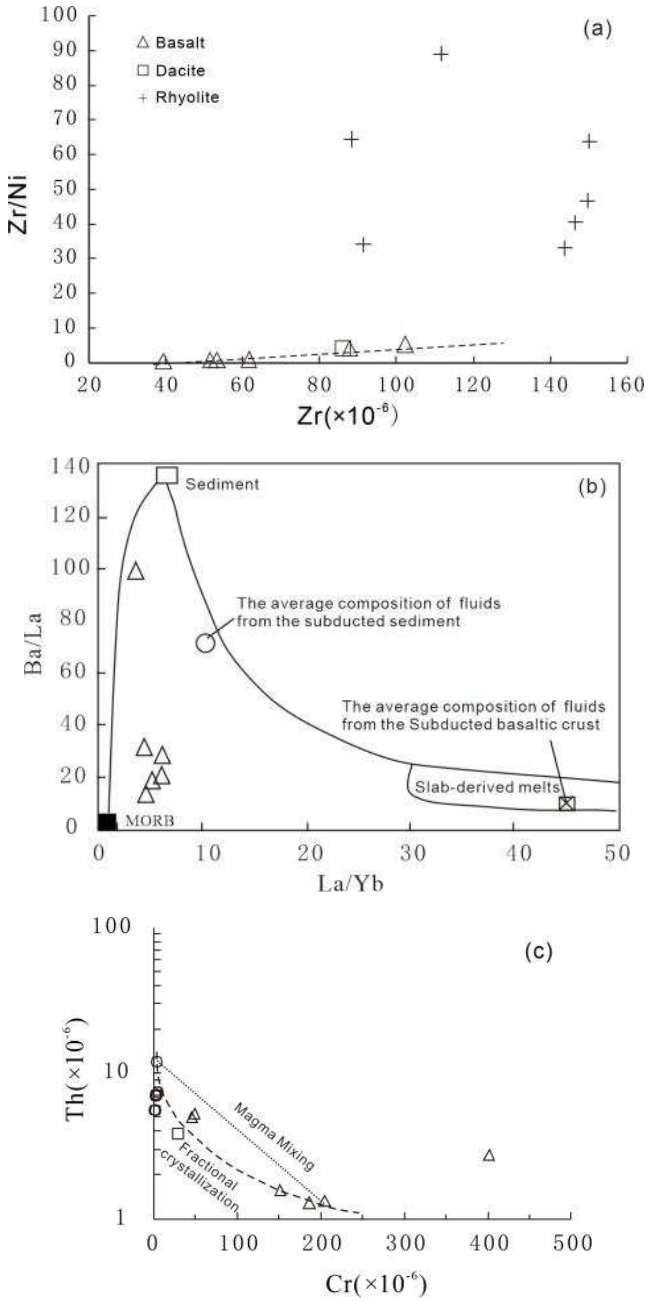

Figure 9. *Zr vs Zr/Ni (after [92]), Ba/La vs La/Yb (after [93]), and Cr vs Th (after [94]) diagrams for the volcanic rocks from Kalamaili.*

7. Conclusions

(1) The Batamayineishan volcanic rocks in Eastern Junggar have complex rock types, with the characteristics of basaltic-andesitic-andesitic-rhyolitic assemblages. They were formed at (319.7±5.9) Ma and ascribed to the products of late Early Carboniferous to early Late Carboniferous.

(2) The Batamayineishan volcanic rocks belong to the high-K calc-alkaline series with typical characteristics of subduction zone volcanic rocks, and formed in the back-arc basin. The basaltic rocks of them may be produced by the partial melting of overlying mantle wedges caused by aqueous fluids from subducted sediments and/or subducted oceanic crust, and have been undergone slightly-moderately fractional crystallization during magma rising. Whereas the acid volcanic rocks are obviously distinct from the basaltic rocks, and they are the result of the interaction between crust-derived magma generated by partial melting of young crust and a small amount of mantle-derived magma, and they have been experienced the strong crystallization differentiation and crustal contamination of mantle basaltic magma in magmatic evolution.

(3) The subduction of the Paleo-Asian Ocean in Eastern Junggar still continued around 320 Ma. Combined with the latest study results, we consider that the final closure time of the Junggar Ocean, an important northern branch of the Paleo-Asian Ocean in Late Paleozoic, should be between 320 Ma and 310 Ma.

(4) The volcanic tectono-magmatism in Eastern Junggar was strong in Carboniferous, with abundant mantle-derived materials involved. As a result, there is a superior metallogenic condition and potential to produce polymetallic deposits associated with subduction in Eastern Junggar, and the Kalamaili has an attractive prospecting prospect.

References

[1] Xiao, X., Tang, Y., & Feng, Y. (1992). Tectonics of Northern Xinjiang and its adjacent areas. Beijing: Geological Publishing House. 1-167.

[2] Xiao, W., Han, C., Yuan, C., Chen, H., Sun, M., & Lin, S. et al. (2006). Unique Carboniferous-Permian tectonic-metalloogenic framework of Northern Xinjiang (NW China): Constraints for the tectonics of the southern Paleoasian Domain. Acta Petrologica Sinica, 22 (5): 1062-1076.

[3] Liu, J., & Xia, Z. (2002). Continental volcanism and Au-Cu metallogenesis in Eastern Junggar, Xinjiang. Beijing Geological Publishing House. 1-225.

[4] Tan, J., Wu, R., Zhang, Y., Wang, S., & Guo, Z. (2009). Characteristics and dating of volcanic rocks of Batamayneshan Formation in Kalameli area, Eastern Junggar. Acta Petrologica Sinica. 25 (3): 539-546.

[5] Yang, P., Gu, S., Zhu, Z., & Feng, Q. (2007). Paleontology and geochemistry study on the radiolarian pebbles from the Lower Jurassic in northeastern the Junggar basin. Journal of Mineralogy and Petrology. 27 (3): 34-38.

[6] Su, Y., Zheng, J., Griffin, W., Tang, H., O Reilly, S., & Lin, X. (2010). Zircon U-Pb and Hf isotopes of volcanic rocks from the Batamayineishan Formation in Eastern Junggar Basin. Chinese Science Bulletin, 55 (36), 4150-4161. doi: 10.1007/ s11434-010- 4151-y.

[7] Su, Y., Zheng, J., Griffin, W., Zhao, J., Tang, H., & Ma, Q. (2012). Geochemistry and geochronology of Carboniferous volcanic rocks in the eastern Junggar terrane, NW China:Implication for a tectonic transition. Gondwana Res, 22 (3-4), 1009-1029. doi: 10.1016/j.gr.2012.01.004.

[8] Li, D., He, D., Santosh, M., & Tang, J. (2014). Petrogenesis of Late Paleozoic volcanics from the Zhaheba depression, East Junggar: Insights into collisional event in an accretionary orogen of Central Asia. Lithos, 184-187, 167-193. doi: 10.1016/j.lithos.2013.10.003.

[9] Luo T, Chen S., Liao Q., Chen J., Hu C., & Wang F., etc. (2016). Geochronology, geochemistry and geological significance of the Late Carboniferous bimodal volcanic rocks in the eastern Junggar. Earth Science, 41 (11): 1845- 1862.

[10] Guo, J., Fan, H., Zhang, S., Liu, X., Wu, T., & Ma, W., et al. (2020). Petrological, He–Ne–Ar and Sr–Nd–Pb geochemical of volcanic rocks constraint on tectonic settings and geodynamic process of the Carboniferous, East Junggar. Journal of Natural Gas Geoscience, 5 (2), 91-104. doi: 10.1016/j.jnggs.2020.02.002.

[11] Zou G, Yu N, Sun G, Huang X, Nijati A., & Lu G. (2021). Geochemical Characteristics and Tectonic Significance of Carboniferous Bimodal Volcanic Rocks in Aoyituolangge Area, Eastern Junggar. Journal of Jilin University (Earth Science Edition), 51 (2): 455-472.

[12] Zhu, Z., Li, S., & Li, GL. (2005). The characteristics of sedimentary system-continental facies volcano in later Carboniferous batamayi group, Zhi-Fang Region, East Junggar. Xinjiang Geology, 23 (1): 14-25.

[13] Zhao, X., Jia C., Zhang, G., Wei, Y.,Lai, S.,& Fang, X. et al. (2008). Geochemistry and tectonic settings of Carboniferous intermediate-basic volcanic rocks in Ludong-Wucaiwan, Junggar basin. Earth Science Frontiers, 15 (2): 272-279.

[14] Mao, Z., Zou, C., Zhu, R., Guo, H., Wang, J., & Tang, Y. et al. (2010). Geochemical characteristics and tectonic settings of Carboniferous volcanic rocks in the Junggar Basin. Acta Petrologica Sinica, 26 (1): 207-216.

[15] Long, X., Sun, M., Yuan, C., Xiao, W., Chen, H., & Zhao, Y. (2006). Genesis of Carboniferous volcanic rock in the Eastern Junggar: constraints on the closure of the Junggar Ocean. Acta Zoologica Sinica, 22 (1): 31-40.

[16] Bian, W. (2011). Volcanic reservoir geological characterization of the Batamayineishan Formation in Junggar Basin. Doctoral Dissertation, 1-81.

[17] Wang, J., Su, Y., Zheng, J., Belousova, E., Chen, M., & Dai, H. (2021). Petrogenesis of early Carboniferous bimodal-type volcanic rocks from the Junggar Basin (NW China) with implications for Phanerozoic crustal growth in Central Asian Orogenic Belt. Gondwana Res, 89, 220-237. doi: 10.1016/j.gr.2020.10.008.

[18] Huang, J., Jiang, C., & Wang, Z. (1990). On the opening-closing tectonics and accordion movement of plate in Xinjiang and adjacent regions. Geoscience of Xinjiang, (1): 3-14.

[19] Wang, D., & Deng, J. (1995). Characteristics and evolution of the plate tectonics in Eastern Jungar, Xinjiang. Journal of Chengdu Institute of Technology, 22 (4): 38-45.

[20] Shu, L., & Wang, Y. (2003). Late Devonian-Early Carboniferous radiolarian fossils from siliceous rocks of the Kalamaili ophiolite, Xinjiang. Geological Review, 19 (4): 408-412.

[21] Li, J., Yang, T., Li, Y., & Zhu, Z. (2009). Geological features of the Kalamaili faulting belt, eastern Junggar region, Xinjiang, China and its constraints on the reconstruction of Late Paleozoic ocean-continental framework of the Central Asian region. Geological Bulletin of China, 28 (12): 1817-1826.

[22] Wang, B., Jiang, C., Li, Y., Wu, H., Xia, Z., & Lu, R. (2009). Geochemistry and tectonic implications of Karamaili ophiolite in Eastern Junggar of Xinjiang. Journal of Mineralogy and Petrology, 29 (3): 74-82.

[23] Zhi, Q., Li, Y., Duan, F., Tong, L., Chen, J., & Gao, J. (2020). Geochemical, Sr-Nd-Pb and zircon U-Pb-Hf isotopic constraints on the Late Carboniferous back-arc basin basalts from the Chengjisihanshan Formation in West Junggar, NW China. Geol Mag, 157 (11), 1781-1799. doi: 10.1017/S0016756820000059.

[24] Yin, J., Yuan, C., Sun, M., Long, X., Zhao, G., & Wong, K. (2010). Late Carboniferous high-Mg dioritic dikes in Western Junggar, NW China: Geochemical features, petrogenesis and tectonic implications. Gondwana Research, 17 (1), 145-152. doi: 10.1016/j.gr. 2009.05.011.

[25] Tang, H., Meng, G., Yang, Y., Deng, Z., Yan, J., & Qi, G. et al. (2018). Geological and geochemical features of the Permian bimodal volcanic rocks in the Qiakurtu Area, Eastern Junggar Basin, Xinjiang, and their tectonic significance. Geoloogical Review, 64 (06): 1393-1412.

[26] Deng, J., Luo, Z., Su, S., Mo, X., Ding, B., & Lai, X. et al. (2009). Petrogenetic tectonic environment and mineralization. Beijing Geological Publishing House. 1-381.

[27] Sun, S., Mcdonough, W., Saunders, A., & Norry, M. (1989). Chemical and isotopic systematics of oceanic basalts: implications for mantle composition and processes. Geological Society Special Publications, 42 (1), 313-345. doi: 10.1144/GSL. SP.1989.042.01.19.

[28] Le Maitre, R., Streckeisen, A., Zanettin, B., Le Bas, M., Bonin, B., & Bateman, P. (2002). Igneous Rocks: A Classification and Glossary of Terms: Recommendations of the International Union of Geological Sciences Subcommission on the Systematics of Igneous Rocks (2nd ed.). Cambridge: Cambridge University Press, 30-42. doi: 10.1017/CBO9780511535581.

[29] Winchester, J., & Floyd, P. (1977). Geochemical discrimination of different magma series and their differentiation products using immobile elements. Chemical Geology, 20: 325-343. doi: 10.1016/0009-2541(77)90057-2.

[30] Rickwood, P. (1989). Boundary lines within petrologic diagrams which use oxides of major and minor elements. Lithos, 22 (4), 247-263. doi: 10.1016/0024-4937(89)90028-5.

[31] Irvine, T., & Baragar, W. (1971). A guide to the chemical classification of the common volcanic rocks. Can J Earth Sci, 8 (5), 523-548. doi: 10.1139/e71-055.

[32] Wilson M. (2007). Igneous Petrogenesis: A global Tectonic Approach. London: Unwin Hymen Ltd, 1-466.

[33] Li, Y., Yang, J., Zhang, J., Li, T., Chen, S., Ren, Y., & Xu, X. (2011). Tectonic significance of the Carboniferous volcanic rocks in eastern Tianshan. Acta Petrologica Sinica, 27 (1): 193-209.

[34] Pearce, J. (1982). Trace element characteristics of Lava from destructive plate boundaries. In: Thorpe R S. ed. Andesites: orogenic andesites and related rocks. New York: John Willey and Sons, v525~548.

[35] Zhang, B. (2021). Geochemical study of continental orogenic belts: on the improvement of geochemical discrimination of tectonic settings of rocks. Northwestern Geology, 34 (3): 1-17.

[36] Depaolo, D., & Wasserburg, G. (1977). The sources of island arcs as indicated by Nd and Sr isotopic studies. Geophys Res Lett, 4 (10), 465-468. doi: 10.1029/GL004i010p00465.

[37] Cui, M., Meng, F., & Wu, X. (2011). Early Ordovician island arc of Qimantag Mountain, eastern Kunlun: Evidence from geochemistry, Sm-Nd isotope and geochronology of intermediate-basic igneous rocks. Acta Petrologica Sinica, 27 (11): 3365-3379.

[38] Dilek, Y., Furnes, H., & Shallo, M. (2008). Geochemistry of the Jurassic Mirdita Ophiolite (Albania) and the MORB to SSZ evolution of a marginal basin oceanic crust. Lithos, 100 (1-4), 174-209. doi: 10.1016/j.lithos.2007.06.026.

[39] Zhang, Y., & Guo, Z. (2010). New constraints on formation ages of ophiolites in Northern Junggar and comparative study on their connection. Acta Petrologica Sinica, 26 (2): 421-430.

[40] Yang, K., Bian, W., Wang, Q., Wang, P., Lang, J., & Li, Z. (2018). Zircon U-Pb age and its geological significance of the igneous rocks from Batamayineishan Formation in East Junggar. Acta Petrologica Sinica, 34 (11): 3341-3358.

[41] Tang, H., Su, Y., Liu, C., Hou, G., & Wang, Y. (2007). Zircon U-Pb age of the plagiogranite in Kalamaili belt, Northern Xinjiang and its tectonic implications. Geotectonica et Metallogenia, 31 (1): 110-117.

[42] Zhou, D., Liu, Y., Xing, X., Hao, J., Dong, Y., & Ouyang, Z. (2006). Formation of the Permian basalts and implications of geochemical tracing for paleo-tectonic setting and regional tectonic background in the Turpan-Hami and Santanghu basins, Xinjiang. Science in China (Series D), 49 (6): 584-596.

[43] Hao, J., Zhou, D., Liu, Y., & Xing, X. (2006). Geochemistry and tectonic settings of Permian volcanic rocks in Santanghu basin, Xinjiang. Acta Petroologica Sinica, 22 (1): 189-198.

[44] Bi C., Yu N., Lu G., Nijiati·A., Pan F., & Mabi Ai. (2019). Redetermination and disintegration of the continental volcanic strata of the former Santanghu Formation in Oetonggar area, Eastern Junggar Basin. Geology in China, 46 (6): 1384-1395.

[45] Rudnick, R. & Gao, S. (2003). The composition of the Continental Crust. Treatise Geochem 3: 1-64. Treatise on Geochemistry (eds. Holland, H. and Turekinan, K.). Elsevier, Oxford, 3: 1-64. doi: 10.1016/B0-08-043751-6/03016-4.

[46] Aldrich, M, Chapin, C., & Laughlin, A. (1986). Stress history and tectonic development of the Rio Grande Rift, New Mexico. Journal of Geophysical Research: Solid Earth, 91 (B6), 6199-6211. doi: 10.1029/JB091iB06p06199.

[47] Xia, L., Xia, Z., Xu, X., Li, X. & Ma, Z. (2007). The discrimination between continental basalt and island arc basalt based on geochemical method. Acta Petrologica et Mineralogica. 26 (1): 77-89.

[48] Su, W., Cai, K., Sun, M., Wan, B., Wang, X., & Bao, Z. (2018). Carboniferous volcanic rocks associated with back-arc extension in the western Chinese Tianshan, NW China: Insight from temporal-spatial character, petrogenesis and tectonic significance. Lithos, 241-254. doi: 10.1016/j.lithos.2018.04.012.

[49] Saunders, A., Storey, M., Kent, R., & Norry, M. (1992). Consequences of plume-lithosphere interaction. Geological Society, London, Special Publications, London, 68: 41-60. doi: 10.1144/GSL.SP.1992.068.01.04.

[50] Kieffer, B., Arndt, N., Lapierre, H., Bastien, F., Bosch, D., & Pecher, A. (2004). Flood and Shield Basalts from Ethiopia: Magmas from the African Superswell. J Petrol, 45 (4), 793-834. doi: 10.1093/petrology/egg112.

[51] Weaver, B., Tarney, J., Pollack, H., & Murthy, V. (1984). Major and trace element composition of the continental lithosphere. Phys Chem Earth, 15, 39-68. doi: 10.1016/0079-1946(84)90004-1.

[52] Wedepohl, K. (1995). The composition of the continental crust. Geochimica et Cosmochimica Acta, 59 (7): 1217-1232. doi: 10.1016/0016-7037(95)00038-2.

[53] Rollinson, H. (1993). Using geochemical data: evaluation, presentation, interpretation. Longnan Group UK Ltd., New York, 1-352. doi: 10.1180/minmag.1994.058.392.25.

[54] Gill, J. (1981). Geophysical Setting of Volcanism at Convergent Plate Boundaries, Orogenic Andesites and Plate Tectonics. Berlin: Springer, 44-63. doi: 10.1007/978-3-642-68012-0.

[55] Li, W, Liu, Y, Dong, Y, Zhou, X, Liu, X, & Li, H. et al. (2012). The geochemical characteristics, geochronology and tectonic significance of the Carboniferous volcanic rocks of the Santanghu area in northeastern Xinjiang, China. Science China: Earth Sciences, 42 (11): 1716-1728.

[56] Deng, J., Xiao, Q., Su, S., Liu, C., Zhao, G., & Wu, Z. et al. (2007). Igneous petrotectonic assemblages and tectonic settings: a discussion. Geological Journal of China Universities, 13 (3): 392-402.

[57] Pearce, J., & Cann, J. (1973). Tectonic setting of basic volcanic rocks determined using trace element analyses. Earth Planet Sc Lett, 19 (2), 290-300. doi: 10.1016/0012-821X (73)90129-5.

[58] Meschede, M. (1986). A method of discriminating between different types of mid-ocean ridge basalts and continental tholeiites with the Nb-Zr-Y diagram. Chem Geol, 56 (3-4), 207-218. doi: 10.1016/0009-2541(86)90004-5.

[59] Pearce, J., Harris, N. & Tindle, A. (1984). Trace element discrimination diagrams for the tectonic interpretation of granitic rocks. Journal of Petrology, 25 (4): 956-983. doi: 10.1093/petrology/25.4.956.

[60] Cabanis, B., & Thieblemont, D. (1988). La discrimination des tholeiites continentales et des basaltes arriere-arc proposition d'un nouveau diagramme, le triangle Th-3xTb-2xTa. Bulletin de la Société Géologique de France, IV (6), 927-935. doi: 10.2113/gssgfbull.IV.6.927.

[61] Pearce, J., & Norry, M. (1979). Petrogenetic implications of Ti, Zr, Y, and Nb variations in volcanic rocks. Contrib Mineral Petr, 69 (1), 33-47. doi: 10.1007/BF00375192.

[62] Wu, X., Liu, D., Wei, G., Li, J. & Li, Z. (2009). Geochemical characteristics and tectonic settings of Carboniferous volcanic rocks from Ludong-Wucaiwan area, the Junggar basin. Acta Petrological Sinica, 25 (1): 55-66.

[63] Tian, L., Castillo, P., Hawkins, J., Hilton, D., Hanan, B, & Pietruszka, A. (2008). Major and trace element and Sr-Nd isotope signatures of lavas from the Central Lau Basin: Implications for the nature and influence of subduction components in the back-arc mantle. J Volcanol Geoth Res, 178 (4), 657-670. doi: 10.1016/j.jvolgeores.2008.06.039.

[64] Randall, A., Martin, R., John, L., Jorge, A., & Lawrence, A. (2002). Geochemistry of back arc basin volcanism in Bransfield Strait, Antarctica: Subducted contributions and along-axis variations. Journal of Geophysical Research: Solid Earth, 107 (B8): EVC4-1-EVC4-17. doi: 10.1029/2001JB000444.

[65] Fretzdorff, S., Livermore, R. A., Devey, C. W., Leat, P. T., & Stoffers, P. (2002). Petrogenesis of the back-arc East Scotia Ridge, South Atlantic Ocean. J Petrol, 43 (8), 1435-1467. doi: 10.1093/petrology/43.8.1435.

[66] Saunders, A., & Tarney, J. (1979). The geochemistry of basalts from a back-arc spreading centre in the East Scotia Sea. Geochim Cosmochim Ac, 43 (4), 555-572. doi: 10.1016/0016-7037(79)90165-0.

[67] Dosso, L., Boespflug, X., Romeur, M., Turpin, L., Calvez, JY., & Bougault, H. (1988). Isotopic and trace element data on Vack-Arc basalts from the South West Pacific Basins and the Sunda Arc. Chemical Geology, 70 (1-2): 47.

[68] Xu, J., Mei, H., Yu, X., Bai, Z., Niu, H., & Chen, F. et al. (2001). Adakites related to subduction in the northern margin of Junggar arc for the Late Paleozoic: Products of slab melting. Chinese Science Bulletin, 46 (8): 684-688.

[69] Zhang, H., Niu, H., Yu, X., Hiroaki, S., Junichi, I., & Shan, Q. (2003a). Geochemical characteristics of the Shaerbulake boninites and their tectonic significance, Fuyun County, Northern Xinjiang, China. Geochimica, 32 (3): 155-160.

[70] Zhang, H., Niu, H., Yu, X., Shan, Q., Hiroaki, S., & Junichi, I. (2003b). Discovery of Nb-Rich basalt at the northeast margin of the Junggar late and the geological sigificance. Discussion on Geological Prospecting, 18 (1): 71-72.

[71] Zhang, H., Niu, H., Hiroaki, S., Shan, Q., Yu, X., & Junichi, I. (2004). Late Paleozoic adakite and Nb enriched basalt from Northern Xinjiang: Evidence for the Southward Subduction of the Paleo-Asian Ocean. Geological Journal of China Universities, 10 (1): 106-113.

[72] Yuan, C., Xiao, W., Chen, H., Li, J., & Sun, M. (2006). Zhaheba potassic basalt, Eastern Junggar (NW China): Geochemical Characteristics and Tectonic Implications. Acta Geologica Sinica, 80 (2): 254-263.

[73] Niu, H., Shan, Q., Zhang, H., & Yu, X. (2007a). $^{40}Ar/^{39}Ar$ geochronoloogy of the ultrahigh-pressure metamorhic quartz-magnesitite in Zaheba, Eastern Junggar, Xinjiang. Acta Petrologica Sinica, 23 (7): 1627-1634.

[74] Niu, H., Zhang, H., Shan, Q., & Yu, X. (2007b). Discovery of supertitanicand supersilicie garnet eclogite in Zhaheba and their geologicalsignificance. Chinese Science Bulletin, 18: 2169-2175.

[75] Niu, H., Shan, Q., Zhang, B., Luo, Y., Yang, W. &Yu, X. (2009). Discovery of garnet amphibolite in Zaheba ophiolitic melange, Eastern Junggar, NW China. Acta Petrologica Sinica, 25 (6): 1484-1491.

[76] Dong, L., Xu, X., Qu, X., & Li, G. (2009). Tectonic setting and formation mechanism of the circum-the Junggar porphyritic copper deposit belts. Acta petrologica Sinica, 25 (4): 713-737.

[77] Gu, P., Li, Y., Wang, X., Zhang, H., & Wang, J. (2010). Geochemical evidence and tectonic significances of Dalabute SSZ-type ophiolitic Mélange, Western Junggar Basin. 57 (1): 36-44.

[78] Xu, X., He, G., Li, H., Ding, T., Liu, X., & Mei, S. (2006). Basic characteristics of the Karamay ophiolitic melange belt and SHRIMP age information of faultstones. Geology of China, 33 (3): 470-475.

[79] Su, Y., Tang, H., & Cong, F. (2008). Zircon U-Pb age and petrogenesis of the Huangyangshan alkalinegranite body in East Junggar, Xinjiang. Acta Mineralogica Sinica, 28 (2): 117-126.

[80] Tang, H., Meng, G., WANG, Z. (2021). Zircon U-Pb geochronology and Lu-Hf isotopic characteristics of alkaline granites in Zhaheba area, East Junggar, Xinjiang, and their geological significance. Geological Review, 67 (1): 67-68.

[81] Plank, T., & Langmuir, C. (1998). The chemical composition of subducting sediment and its consequences for the crust and mantle. Chem Geol, 145 (3), 325-394. doi: 10.1016/S0009-2541(97)00150-2.

[82] Edwards, C., Menzies, M., Thirlwall, M., Morris, J., Leeman, W., & Harmon, R. (1994). The transition to potassic alkaline volcanism in island arcs: the Ringgit-Beser Complex, East Java, Indonesia. J Petrol, 35 (6), 1557-1595. doi: 10.1093/petrology/35.6.1557.

[83] Turner, S., Foden, J., George, R., Evans, P., Varne, R., Elburg, M., & Jenner, G. (2003). Rates and processes of potassic magma evolution beneath Sangeang Api Volcano, East Sunda Arc, Indonesia. J Petrol, 44 (3): 491-515. doi: 10.1093/petrology/44.3.491.

[84] Wyman, D., Ayer, J., & Devaney, J. (2000). Niobium-enriched basalts from the Wabigoon subprovince, Canada: evidence for adakitic metasomatism above an Archean subduction zone. Earth Planet Sc Lett, 179 (1), 21-30. doi: 10.1016/S0012-821X(00)00106-0.

[85] Hollings, P. (2002). Archean Nb-enriched basalts in the northern Superior province. Lithos, 64: 1-14. doi: 10.1016/S0024- 4937(02)00154-8.

[86] Castillo, P. (2004). Geochemical Constraints on Possible Subduction Components in Lavas of Mayon and Taal Volcanoes, Southern Luzon, Philippines. J Petrol, 45 (6), 1089-1108. doi: 10.1093/petrology/egh005.

[87] Defant, M. J., & Drummond, M. S. (1990). Derivation of some modern arc magmas by melting of young subducted lithosphere. Nature (London), 347 (6294), 662-665. doi: 10.1038/347662a0.

[88] Rapp, R., & Watson, E. (1995). Dehydration melting of metabasalt at 8-32 kbar: implications for continental growth and crust-mantle recycling. J Petrol, 36 (4): 891-931. doi: 10.1093/petrology/36.4.891.

[89] Chen, B., & Arakawa, Y. (2005). Elemental and Nd-Sr isotopic geochemistry of granitoids from the West Junggar foldbelt (NW China), with implications for Phanerozoic continental growth. Geochim Cosmochim Ac, 69 (5), 1307-1320. doi: 10.1016/j.gca.2004.09.019.

[90] Chen, J., Han, B., & Zhang, L. (2010). Geochemistry, Sr-Nd isotopes and tectonic implications of two generations of Late Paleozoic plutons in northern West Junggar, Northwest China. Acta Petrologica Sinica, 26 (8): 2317-2335.

[91] Hong, D., Wang, S., Xie, X., Zhang, J., & Wang, T. (2003). Metallogenic province Derived from mantle Sources: a case study of Central Asian Orogenic Belt. Mineral Deposits. 22 (1): 41-54.

[92] Huang, F., & Jiang, C. (2006). Study on Tengchong volcano. Kunming: Yunnan Science and Technology Press, 96-110.

[93] Zhu, D., Pan, G., Mo, X., Wang, L., Liao, Z., & Zhao, Z. et al. (2006). Late Jurassic-Early Cretaceous geodynamic setting in middle-northern Gangdese: New insights from volcanic rocks. Acta Petrologica Sinica, 22 (3): 534-546.

[94] Xia, L., Xia, Z., Xu, X., Li, X., Ma, Z., & Wang, L. (2005). Relationships between basic and silicic magmatism in continental rift settings: a petrogeochemical study of the Carboniferous post-collisional rift silicic volcanics in the Tianshan, NW China. Acta Geologica Sinica, 79 (5): 633-353.